https://doi.org/10.5194/egusphere-2026-519
Preprint. Discussion started: 4 February 2026


# Holocene methane pockmarks in the Baltic Sea, Part I: Archaeal community composition based on tetraether lipids and 16S rRNA analysis

Izabela De Mey-Śnieżyńska[1*], Mirosław Słowakiewicz[1], Francien Peterse[2], Aleksandra Brodecka-Goluch[4], Andrzej Borkowski[3], Katarzyna Łukawska-Matuszewska[4]

[1]University of Warsaw, Faculty of Geology, 02-089 Warsaw, Poland

[2]Utrecht University, Department of Earth Sciences, 3584 CS Utrecht, The Netherlands

[3]AGH University of Krakow, Faculty of Geology, Geophysics and Environmental Protection, 30-059 Kraków, Poland

[4]University of Gdańsk, Faculty of Oceanography and Geography, 81-379 Gdynia, Poland

*Corresponding author: i.sniezynska@uw.edu.pl

## Highlights

Pockmark sediments harbour substantially higher archaeal diversity and abundance compared with non-pockmark reference sediments.

Pockmarks appear to function as tightly coupled metabolic systems, in which various archaeal groups potentially cooperate in methanogenesis and ammonia oxidation, whereas non-pockmark sites contain less integrated, loosely coupled sub-communities.

The MET4 pockmark in the Gdańsk Deep hosts the most diverse and abundant methanogen community, coinciding with the highest concentrations of isoprenoid glycerol dialkyl glycerol tetraether lipids (iGDGTs).

Crenarchaeol is the dominant iGDGT in both methane-pockmark and non-pockmark reference sediment cores, likely derived from abundant *Ca.* Nitrosopumilus.

## Abstract

Methane-rich pockmarks and shallow gas systems are prominent geomorphological features in the Baltic Sea that act as hotspots of microbial activity. Methane pockmarks in the Gdańsk Basin differ in seepage intensity, the efficiency of internal methane biofilters, and the influence of freshwater infiltration. The objective of this research was to examine the effects of methane seepage and submarine groundwater discharge (SGD) on the composition of archaeal communities and the archaeal tetraether lipids (GDGTs) produced by these communities across the examined gas systems. Additionally, the research assessed how these environmental factors affect the use and interpretation of GDGT-based proxies in such environments. The study investigates whether GDGT patterns in these gas systems primarily reflect methane-driven processes (anaerobic oxidation of methane and methanogenesis) or ammonia oxidation, which is a key process in the Baltic Sea. It also evaluates how reliably GDGT indices can be applied in this dynamic environment characterised by strong upward gas flow. The results show elevated GDGT concentrations in pockmark sediments compared with reference non-pockmark sediments; however, GDGT concentrations are variable and depend on whether the flow is active or inactive, reflecting episodic submarine groundwater discharge that coincides with

https://doi.org/10.5194/egusphere-2026-519
Preprint. Discussion started: 4 February 2026


methane release. Overall, GDGT concentrations are much higher at sites with minimal or no SGD. Nevertheless, consistently low Methane Index values (MI < 0.09), together with low GDGT-0/crenarchaeol (< 1) and GDGT-2/cren (< 0.04) ratios, indicate that the iGDGT patterns lack the typical enrichment associated with methane-rich and anaerobic oxidation of methane (AOM) settings, suggesting no strong AOM imprint on the GDGT pool. OH-GDGT% values are consistent with those of Baltic Sea surface sediments. GDGT-based proxies in this system, therefore, primarily reflect ammonia-oxidiser activity rather than methane flux. These findings highlight the complex interplay between SGD and methane fluxes in shaping archaeal communities, GDGT composition, and their sedimentary record. GDGT-based indices must be applied with caution in dynamic shallow gas systems.

**Keywords:** methane, pockmarks, iGDGTs, ammonia-oxidising archaea, crenarchaeol, Holocene, Gdańsk Deep, Baltic Sea

## 1 Introduction

Pockmarks are concave geological structures ranging from 1 to over 100 m in width and from less than 1 to 100 m in depth, formed worldwide by fluid discharge from the lithosphere to the hydrosphere (King and MacLean, 1970; Hovland and Judd, 1988). As indicators of hydraulic activity, they are categorised as active or inactive depending on whether fluid emanation is continuous or dormant/intermittent (Hovland and Judd, 1988; Hovland et al., 2002). Their seabed depressions facilitate detection by geophysical and hydroacoustic surveys, making them practical proxies for investigating seepage phenomena (Hovland and Judd, 1988). Formation of pockmarks requires pressure build-up in fine-grained, low-permeability sediments, with methane being the most commonly emitted component owing to its high mobility (Hovland and Judd, 1988). Fluid types vary globally and include biogenic, thermogenic, or hydrothermal gas, groundwater, or combined gas-and-water seepage (Hovland and Judd, 1988). Pockmarks predominantly form along salt-dome margins (Schmuck and Paull, 1993; Taylor et al., 2000) and in dislocation zones, faults, and bedrock fractures (Shaw et al., 1997), although they also occur in regions of low seismicity, such as Sweden (Hovland et al., 2002) and the southern Baltic Sea (Idczak et al., 2020). Glacial and post-glacial processes can influence their formation by generating overpressure, as observed in the North Sea (Callow et al., 2021) and the Baltic Sea (Whiticar and Werner, 1981; Whiticar, 2002; Kreuzburg et al., 2023).

Baltic Sea pockmarks have been documented in Eckernförde Bay and the Mecklenburg Bight (Werner, 1978; Wever et al., 1998; Jensen et al., 2002; Schlüter et al., 2004; Hoffmann et al., 2020; Díaz-Mendoza et al., 2023), the Stockholm Archipelago (Jakobsson et al., 2020), offshore Finland (Virtasalo et al., 2019), and the Gdańsk Basin (Pimenov et al., 2010; Majewski and Klusek, 2011; Brodecka et al., 2013; Jaśniewicz et al., 2019; Idczak et al., 2020; Brodecka-Goluch et al., 2022), which is the focus of this study.

In several Baltic settings, pockmarks are linked to submarine groundwater discharge (SGD), i.e., freshwater groundwater and/or recirculated seawater flow across the seabed driven by hydraulic and density-related pressure gradients (Burnett et al., 2003, 2006; Moore, 2010; Taniguchi et al., 2019) – including those in Eckernförde Bay (Bussmann and Suess, 1998; Schlüter et al., 2004), Hanko Bay (Virtasalo et al., 2019; Purkamo et al., 2022), and the central Gulf of Gdańsk (Szymczycha et al., 2016; Idczak et al., 2020).

https://doi.org/10.5194/egusphere-2026-519
Preprint. Discussion started: 4 February 2026


Submarine groundwater discharge affects methane pockmarks by driving cyclical activity (from initiation through expansion to stabilisation) and turbulent mixing that disturbs water-column stratification, resuspends sediments, and can, in effect, modify porewater chemistry (Zhang et al., 2025). Pockmark depressions trap biological, marine, and terrestrial material and objects (e.g., boulders, plastic bags), acting as sediment traps (Rise et al., 2014; Idczak et al., 2020). Under such conditions, freshening of porewater and near-bottom water can induce shallow methanogenesis and trigger episodic gas release (Moore, 2010; Idczak et al., 2020). SGD influences $NH_4^+$, $CH_4$, dissolved inorganic carbon (DIC), and $H_2S$ concentrations (Schlüter et al., 2004; Liu et al., 2017; Idczak et al., 2020; O'Reilly et al., 2021; Brodecka-Goluch et al., 2022; Zhang et al., 2025) and alters porewater chemistry through decreased salinity and chloride depletion (Schlüter et al., 2004), controlled by shifting advective and diffusive/dispersive flow dynamics (Purkamo et al., 2022). Advection flushes sediments, pushes reaction zones towards the surface, and decreases methane accumulation by restricting organic-matter build-up and shifting microbial communities (Purkamo et al., 2022). Freshwater infiltration reduces sulphate availability and weakens sulphate-driven anaerobic oxidation of methane (S-AOM), which is critical in low-salinity basins such as the Baltic Sea (Idczak et al., 2020; Brodecka-Goluch et al., 2022).

In methane-bearing sediments, sulphate and methane diffuse in opposite directions and meet at the sulphate-methane transition zone (SMTZ), where microbial communities carry out anaerobic oxidation of methane (AOM) (Zehnder and Brock, 1980; Boetius et al., 2000). This process is mediated by sulphate-reducing bacteria (SRB) and anaerobic methanotrophic archaea (ANME) (Knittel and Boetius, 2009), which consume methane before it reaches the sediment-water interface, thereby limiting transfer to the overlying water column and mitigating atmospheric emissions (Reeburgh, 2007). In the Baltic Sea, a permanent halocline at depths of 60-80 m creates a redoxcline that separates oxygenated upper waters from oxygen-depleted lower layers and structures multiple biogeochemical cycles (Kuliński et al., 2022), including an oxic-suboxic zone of nitrogen cycling in which ammonia-oxidising archaea (AOA) play a crucial role (Berg et al., 2015b; Jäntti et al., 2018). Biomarkers of archaea involved in both methane-related processes (ANME, methanogens) and nitrification (AOA) can be preserved in sediments as diagnostic membrane-lipids – namely isoprenoidal glycerol dialkyl glycerol tetraethers (iGDGTs) – which may be transported and buried in sediments, potentially biasing GDGT-based proxies (Schouten et al., 2013).

iGDGTs are membrane lipids uniquely synthesised by archaea, in which cyclisation and hydroxylation regulate membrane properties in response to environmental conditions (De Rosa et al., 1977; Huguet et al., 2006; Liu et al., 2017; Schouten et al., 2002, 2013; Sinninghe Damsté et al., 2022). In marine sediments, GDGT-0 and crenarchaeol are dominant (Schouten et al., 2000, 2002). Crenarchaeol is produced by Thaumarchaeota (Sinninghe Damsté et al., 2022) – in current nomenclature, Nitrososphaerota (Rinke et al., 2021) – which are the dominant ammonia oxidisers and iGDGT producers in the Baltic Sea (Labrenz et al., 2010; Berg et al., 2015a, b; Wittenborn et al., 2023). Methanogens primarily produce GDGT-0, whereas methanotrophs, especially ANME-1, produce GDGT-1 to -3 (Koga et al., 1993; Pancost et al., 2001; Weijers et al., 2006; Rossel et al., 2008; Blaga et al., 2009; Zhang et al., 2011; Inglis et al., 2015; Słowakiewicz et al., 2016; Petrick et al., 2019). Hydroxylated-GDGTs (OH-GDGTs) contain additional hydroxyl groups and varying numbers of cyclopentane rings and are produced primarily by Thaumarchaeota (Sinninghe Damsté et al., 2002; Liu et al., 2012; Kaiser and Arz, 2016; Elling et al., 2017; Bale et al., 2019; Sinninghe Damsté et al., 2022), although methylotrophic methanogens or ANME may contribute during the formation of methane-seep carbonates (Liu et al., 2012; Guan et al., 2024). OH-GDGT synthesis reflects cold adaptation,

https://doi.org/10.5194/egusphere-2026-519
Preprint. Discussion started: 4 February 2026


making these compounds useful temperature proxies (Liu et al., 2012). These are also sensitive to salinity, as lower salinity promotes the formation of additional cyclopentane rings (Sinninghe Damsté et al., 2022). OH-GDGT-0 dominates at higher latitudes (Huguet et al., 2013; Varma et al., 2024) and recent Baltic Sea sediments (Sinninghe Damsté et al., 2022), where culture studies confirmed an AOA source (Blainey et al., 2011; Berg et al., 2015a).

South-eastern Baltic Sea sediments release approximately ~$280 \times 10^6$ mmol of methane per day (Ulyanova et al., 2012). While methane seeps globally enhance microbial dynamics and biodiversity (Ruff et al., 2015; Carrier et al., 2020), the Baltic Sea is strongly stratified, and its persistent redox gradients favour intense pelagic nitrification and a widespread AOA community whose biomass and lipids can be exported to the seafloor. Accordingly, ammonia oxidation is prominent in the Baltic Sea, with *Candidatus* Nitrosopumilus being widespread and well adapted to suboxic conditions along redox gradients (Labrenz et al., 2010; Berg et al., 2015b; Wittenborn et al., 2023). However, the relative contributions of methane-driven benthic sources and pelagic AOA export to sedimentary iGDGT distributions in Baltic pockmarks remain poorly constrained. In this study, it is hypothesised that pockmark sediments, as hotspots of AOM and methanogenesis, display iGDGT distributions reflecting a greater contribution from methane-cycling archaea (methanogens and anaerobic methanotrophs), whereas non-pockmark sediments exhibit mixed signatures with a stronger pelagic AOA influence. Because GDGTs are taxon-linked, iGDGT patterns can serve as proxies for archaeal community composition (AOA versus methanogens/ANME), providing insights into community structure. This hypothesis is tested by comparing iGDGT distributions and total organic carbon (TOC) content in sediment cores from pockmark and non-pockmark areas, complemented by archaeal 16S rRNA gene metabarcoding, to evaluate whether lipid sources correspond to shifts in archaeal community composition.

## 2 Materials and methods

### 2.1 Study area

Pockmarks in the Gdańsk Deep and the central Gulf of Gdańsk (Fig. 1) occur at water depths of 1-100 m and are characterised by active gas seepage from Holocene silts and clays (Idczak et al., 2020). Although the gas is predominantly biogenic (Brodecka-Goluch et al., 2022), the presence of helium (up to 0.39%) (Idczak et al., 2020) and noble gases (Ne, Ar, Kr, Xe) (Brodecka-Goluch et al., 2022) in samples from station MET1 suggests that these pockmarks vent Middle Cambrian reservoirs, with gas migrating through sedimentary layers along faults (Jaworowski et al., 2010; Idczak et al., 2020; Brodecka-Goluch et al., 2022), possibly with additional crustal and mantle contributions (Kotarba, 2010; Pokorski, 2010; Kotarba and Lewan, 2013; Kotarba and Nagao, 2015).

The study area spans the Gdańsk Basin and includes stations MET3 and MET4 in the northern Gdańsk Deep, and MET1-MP and MET1-BH in the Gulf of Gdańsk (Fig. 1). The southern stations (MET1 area) receive high inputs of terrestrial organic matter from the Vistula River, trap plant material in pockmarks, and experience moderate anthropogenic contamination, resulting in elevated TOC (Idczak et al., 2020; Łukawska-Matuszewska et al., 2022; Szymczak-Żyła and Lubecki, 2022). The northern stations (MET3, MET4) receive less terrestrial input and are dominated by marine organic matter (Brodecka-Goluch et al., 2022). Sedimentation rates are lower in MET3 and MET4 (~0.17–0.20 cm $yr^{-1}$) than at MET1 (~0.15–0.22 cm $yr^{-1}$) (Szczepańska and Uścinowicz, 1994; Brodecka-Goluch et al., 2022). The MET1 pockmarks are characterised by methane bubbling and submarine groundwater discharge (Idczak et al., 2020;

https://doi.org/10.5194/egusphere-2026-519
Preprint. Discussion started: 4 February 2026


Brodecka-Goluch et al., 2022). Methanogenesis pathways vary between sites: acetoclastic at MET1-BH, hydrogenotrophic at MET3, and mixed at MET1-MP (Idczak et al., 2020; Brodecka-Goluch et al., 2022). MET4 represents a stable, non-ebullitive and least-studied system (Brodecka et al., 2013).

In the Gdańsk Basin, SGD is divided into shallow/coastal and deep/offshore components. The shallow/coastal component occurs in nearshore areas and is fed by Quaternary-Cretaceous coastal aquifers (e.g., Piekarek-Jankowska, 1996; Szymczycha et al., 2016, 2018), whereas the deep/offshore component comprises artesian-type freshwater seepage with episodic discharge at deep-water pockmarks such as MET1 (Szymczycha et al., 2018; Idczak et al., 2020). Deep SGD originates from extensive Upper Cretaceous aquifers beneath the Gulf of Gdańsk (Uścinowicz, 2011). Seepage intensity varies with hydrostatic pressure, water-column processes, and fault activity (Brodecka-Goluch et al., 2022). After commercial extraction ceased in 2000, natural hydrodynamic conditions returned (Uścinowicz, 2011), although the extent and periodicity of deep discharge remain unquantified. SGD in the MET1 area reduces sulphate and chloride concentrations with depth, compressing the SMTZ to a few cm below the seafloor (Idczak et al., 2020; Brodecka-Goluch et al., 2022; Łukawska-Matuszewska and Dwornik, 2025). A high carbonate alkalinity flux at MET1-MP indicates substantial DIC generation during anaerobic diagenesis, potentially associated with Fe(III)-AOM (Łukawska-Matuszewska and Dwornik, 2025).

### 2.2 Sampling at MET stations

The research stations were divided into pockmarks (sediments containing large amounts of gas and possible SGD) and non-pockmarks (reference sites with gas in the sediments but without emissions to the water column or SGD). Pockmark stations were further classified, based on hydroacoustic and geophysical studies (Idczak et al., 2020; Brodecka-Goluch et al., 2022), as active (gas emission, freshwater seepage, or both: P/MET1-BH, P/MET1-MP, P/MET4) or inactive (gas present in the sediments without clear emission or freshwater seepage: P/MET3).

Eight sediment cores (95 cm long) were obtained from the central parts of methane-seeping structures in the central Gdańsk Basin (south-eastern Baltic Sea) using a gravity corer from three areas and four study locations (MET1: MET1-MP, MET1-BH; MET3; MET4; Fig. 1, supplementary material Table S1) during a cruise aboard RV *Oceanograf* (University of Gdańsk) in October 2019. Four additional cores were collected from outside the pockmarks (~100 m away) as reference samples. Samples were categorised by origin: a ‘P’ prefix (P/METX; X = 1-MP, 1-BH, 3, 4) for pockmark sediments and ‘S’ prefix (S/METX) for surrounding sediments, namely reference non-pockmarks.

Onboard, the 95 cm cores for biomarker analysis were sectioned into a top 0-5 cm interval and subsequent 10 cm intervals (hereafter referred to as horizons) for the remainder of the cores, yielding 72 samples for geochemical analysis (some bottom samples are missing). Samples for microbial analysis were subsampled at a slightly coarser resolution than 10 cm from the top, mid-depth, and bottom intervals using a sterile spatula.

https://doi.org/10.5194/egusphere-2026-519
Preprint. Discussion started: 4 February 2026


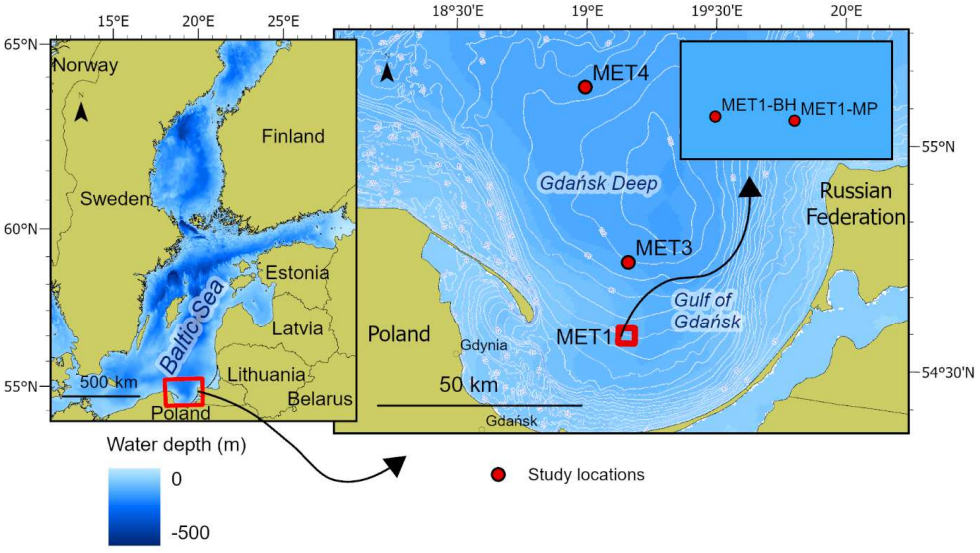


Fig. 1. Map of the study area in the south-eastern Baltic Sea, Gdańsk Basin. Study locations are indicated by red dots. Reference stations (labelled as surroundings and tagged with an "S" prefix) were positioned approximately 100 m away from each of the four pockmark stations on the seafloor, which contain shallow gas within marine sediments but lack seabed features such as pockmarks. Map source: Eurostat/GISCO, 2024, scale 1:1M, EPSG:4326 (CNTR_RG_01M_2024_4326; © EuroGeographics); HELCOM (BSBD, 500 m); PGI-NRI/CBDG, Bathymetric map of the South Baltic Sea, 1:200,000 (OGC WMS 1.3.0).

### 2.3 TOC analysis

The organic matter content was assessed following dehydration (105 °C for 24 h) and dry combustion (550 °C for 6 h) using gravimetric loss-on-ignition (LOI). TOC was estimated from LOI using the empirically derived relationship for Bay of Gdańsk sediments reported by Łukawska-Matuszewska et al. (2014): TOC (wt%) = 0.6042 + 0.3184 × LOI (%). Because LOI-based conversions are sensitive to ignition conditions and sediment composition, and therefore provide a screening-level estimate of TOC rather than an exact measurement, the LOI-derived TOC values were evaluated against directly measured TOC for two representative cores using paired comparisons (1:1 plots and Bland-Altman agreement analysis). Given the limited number of paired measurements, LOI-derived TOC is used qualitatively (at the trend-level) to provide geochemical context rather than for biomarker normalisation.

### 2.4 Tetraether lipid extraction and analysis

All freeze-dried samples were ground using a mortar and pestle. Approximately 1 g of each sample was extracted with dichloromethane:methanol (DCM:MeOH, 2:1, v/v) in an ultrasonic water bath. Total lipid extracts (TLEs) were separated on a silica gel column using *n*-hexane and methanol as eluents to obtain apolar and polar fractions, respectively.

https://doi.org/10.5194/egusphere-2026-519
Preprint. Discussion started: 4 February 2026


The polar fraction containing core GDGTs was re-dissolved in hexane/isopropanol (99:1, v/v), spiked with a known amount of an internal standard (a $C_{46}$ glycerol trialkyl glycerol tetraether; Huguet et al., 2006), and passed through a 0.45 µm polytetrafluoroethylene syringe filter. GDGTs were analysed using an ultra-high-performance liquid chromatograph (UHPLC; Agilent 1260 Infinity) coupled to an Agilent 6130 single-quadrupole mass detector at Utrecht University, following the method proposed by Hopmans et al. (2016). Quantification was based on integrating the peak areas of the protonated ions ($[M+H]^+$) in ChemStation software (B.04.03) and comparing them with those of the internal standard. Selected ion monitoring (SIM) was applied to detect and identify GDGTs. The target ions included *m/z* 1302, 1300, 1298, 1296 and 1292 for iGDGTs and OH-GDGTs. iGDGT data (raw peak areas, derived fractional abundances/indices, and absolute concentrations) are reported in accordance with the archiving and reporting recommendations of Bijl et al. (2025).

### 2.5 DNA isolation, sequencing, and data analysis

Genomic DNA from the sediment samples was isolated using the EURx kit for complex matrices (Soil DNA Purification Kit, no. E3570, EURX Ltd., Poland). The protocol requires mechanical homogenisation of the samples to release cells from the sediment matrix. The isolated genomic DNA was subjected to metabarcoding analysis. Sequencing of the hypervariable V3–V4 region of the 16S rRNA gene was commissioned to GENOMED S.A. (Warsaw, Poland). Specific primer sequences (developed by Zymo Research, CA, USA) were used to amplify the selected region and prepare libraries (341F: CCTACGGGDGGCWGCAG, CCTAYGGGGYGCWGCAG; 806R: GACTACNVGGGTMTCTAATCC).

PCR was performed using Q5 Hot Start High-Fidelity 2× Master Mix, with reaction conditions following the manufacturer's recommendations. Sequencing was conducted on a MiSeq sequencer using paired-end (PE) technology (2 × 300 nt) with Illumina's v3 kit. FASTQ files were processed with *fastp* (v. 0.23.2) (Chen et al., 2018) to improve the quality of the raw sequences by trimming adapters, filtering low-quality reads, and removing artefacts. The sequences were further analysed using Kraken2 (Wood et al., 2019) according to the protocol described by (Lu et al., 2022). The SILVA database (v. 138) was used for taxonomic assignment (Quast et al., 2013). Bracken was then applied to the Kraken2 reports, set at the genus level with a threshold of five (Lu et al., 2017). The resulting data were transformed before analysis. To address zero values, the results were imputed using the R package *Compositions* (v. 1.4.0.1) (Palarea-Albaladejo and Martín-Fernández, 2015). The centred log-ratio (clr) transformation was then applied using the *Compositions* (v. 2.0-5) package for R (Aitchison, 1982; Quinn et al., 2019; van den Boogaart et al., 2024).

### 2.6 Statistical analysis and data visualisation

Multidimensional analyses, correlograms, and hierarchical analyses were performed using R (R Core Team, 2023). RStudio 2025.05.0+496 "Mariposa Orchid", with R version 4.3.3 (2024-02-29) running on the x86_64-apple-darwin20 (64-bit) platform, was used for all analyses. A heatmap with cluster analysis of the archaeal community (at the class taxonomic level) was generated using the Heatmap function from the *ComplexHeatmap* package. To examine the grouping of samples between pockmark and reference sites, Classical Multidimensional Scaling (MDS; principal coordinates analysis) was carried out using dist (dist_matrix <- dist(data), method = "euclidean") and cmdscale (mds <- cmdscale(dist_matrix)) from the *stats* package. The MDS results were visualised using the *ggplot2* and *ggrepel* packages (Wickham, 2016).

https://doi.org/10.5194/egusphere-2026-519
Preprint. Discussion started: 4 February 2026


Permutational Multivariate Analysis of Variance (PERMANOVA) was performed using adonis2 (permutations = 999, method = "bray") from the *vegan* package. Principal Component Analysis (PCA) was conducted using PCA from the *FactoMineR* package, and the results were visualised with fviz_pca_var from the *factoextra* package. A correlation network illustrating relationships between Archaea (at the family taxonomic level) and GDGTs was constructed using cor from the *stats* package; graph_from_adjacency_matrix (mode = "undirected", weighted = TRUE, diag = FALSE) from the *igraph* package; mutate_as_tbl from the *tidygraph* package; and *ggraph* for visualisation. Community structure was identified using group_louvain (multilevel optimisation of modularity via igraph::cluster_louvain()), which implements the multi-level modularity optimisation algorithm described by Blondel et al. (2008). Pairwise correlations among iGDGT concentrations were calculated in R using stats::cor.test() (Pearson and Spearman). Concentrations were $\log_{10}$-transformed before correlation analysis ($\log_{10}[x + 10^{-6}]$) to reduce right skew. Correlations were computed using pairwise complete observations, with the number of paired samples ($n$) reported. To account for multiple testing, $p$-values were adjusted using the Benjamini–Hochberg false discovery rate (FDR) procedure.

### 2.7 Calculation of indices

The GDGT-0/crenarchaeol ratio was calculated to assess potential contributions from methanogens (although GDGT-0 is not exclusive to them) and ammonia-oxidising archaea to iGDGT production (Blaga et al., 2009). Values > 2 have been proposed to indicate a substantial methanogenic input (Blaga et al., 2009; Schouten et al., 2013; Zell et al., 2014).

GDGT-0/cren = [GDGT-0] / [crenarchaeol]

The GDGT-2/crenarchaeol (GDGT-2/cren) index is used as an additional screening tool for a potential AOM contribution (Weijers et al., 2011). An elevated GDGT-2/cren ratio suggests increased synthesis of GDGT-2 within the SMTZ, likely originating from methanotrophic Euryarchaeota (Pancost et al., 2001; Wakeham et al., 2003; Stadnitskaia et al., 2005).

GDGT-2/cren = [GDGT-2] / [crenarchaeol]

The Methane Index (MI) is based on GDGT-1 to GDGT-3 and crenarchaeol and reflects the balance between methanotrophic Euryarchaeota and planktonic or benthic Nitrososphaeria (Zhang et al., 2011). GDGTs associated with methanotrophs — mainly GDGT-1 to GDGT-3 (Pancost et al., 2001; Zhang et al., 2011) — are primarily produced by ANME-1 (Rossel et al., 2008). The MI, defined by Zhang et al. (2011), was calculated as follows:

MI = [GDGT-1 + GDGT-2 + GDGT-3] / [GDGT-1 + GDGT-2 + GDGT-3 + cren + cren′]

The percentage of OH-GDGTs expresses the relative contribution of hydroxylated iGDGTs to the total iGDGT pool and indicates an enhanced contribution from OH-GDGT–producing archaea and/or adaptation to low temperature and salinity. The index was calculated according to Huguet et al. (2013):

OH-GDGT% = Σ[OH-GDGT-0 + OH-GDGT-1 + OH-GDGT-2] / {Σ[OH-GDGT-0 + OH-GDGT-1 + OH-GDGT-2] + Σ[GDGT-0 + GDGT-1 + GDGT-2 + GDGT-3 + cren + cren′]} × 100

https://doi.org/10.5194/egusphere-2026-519
Preprint. Discussion started: 4 February 2026


The ring indices of hydroxylated tetraethers (RI-OH and RI-OH′) quantify the degree of cyclisation, that is, the number of cyclopentane rings in the molecules, which increases with temperature and decreases with salinity (Sinninghe Damsté et al., 2022). The RI-OH′ is more sensitive in cold regions (Varma et al., 2024). The indices were calculated according to Lü et al. (2015):

RI-OH = {[OH-GDGT-1] + 2 × [OH-GDGT-2]} / {[OH-GDGT-1] + [OH-GDGT-2]}
RI-OH′ = {[OH-GDGT-1] + 2 × [OH-GDGT-2]} / Σ[OH-GDGTs]

## 3 Results

### 3.1 LOI-derived TOC

TOC estimated from LOI showed a moderately positive correlation with directly measured TOC (Supplementary material Fig. S1) (MET1-MP: Pearson $r = 0.684$, n = 7, $p = 0.090$; MET3: $r = 0.411$, n = 10, $p = 0.239$), although the small sample size limits statistical power (both $p > 0.05$ at $\alpha = 0.05$). Consequently, LOI-based TOC estimates are interpreted qualitatively (at the trend level), and agreement is assessed mainly through Bland–Altman bias and limits of agreement (supplementary material Fig. S2).

### 3.2 iGDGTs in pockmark and non-pockmark marine surface sediments

The abundance and distribution of iGDGTs (GDGT-0 to GDGT-3, crenarchaeol, and its isomer) were analysed in pockmark sediments and surrounding non-pockmark reference sediments (Fig. 2), and all targeted iGDGTs were detected in both settings. Summed iGDGT concentrations (ΣiGDGTs) span 0.02–58.85 μg $g^{-1}$ sediment across all samples, with values generally higher in pockmarks (0.92–58.85 μg $g^{-1}$ sediment; median 5.10 μg $g^{-1}$; mean 10.58 μg $g^{-1}$) than in reference sediments (0.02–16.81 μg $g^{-1}$ sediment; median 2.59 μg $g^{-1}$; mean 3.73 μg $g^{-1}$), that is, approximately twice as high at the median and three times higher on average.

Spatially, ΣiGDGTs are highest at the Gdańsk Deep study locations (MET3–MET4) and lower in the MET1 area, consistent with an overall increase from south to north, whereas the dominance pattern of crenarchaeol and GDGT-0 remains similar across settings. With depth, ΣiGDGTs often show shallow to mid-depth maxima (commonly 15–45 cm), followed by downcore depletion; concentrations typically decline by a factor of ~2.6 to ~64, and can appear much larger (up to ~840-fold) where values approach near-zero in the deepest reference intervals (S/MET4). When normalised to TOC, iGDGT concentrations remain higher in pockmark sediments than in non-pockmark sediments (Fig. 2), although this difference is less pronounced than when expressed per gram of sediment. However, LOI-derived TOC captures only the broad downcore trend (declining with depth) and shows core-dependent uncertainty; therefore, it is used solely to provide geochemical context (Fig. 2, supplementary material Fig. S1, S2).

Crenarchaeol is the dominant iGDGT in both pockmark sediments (fractional abundance, FA = 0.53 ± 0.03 SD) and non-pockmark sediments (0.55 ± 0.02 SD), followed by GDGT-0 (FA = 0.43 ± 0.03 SD in pockmarks and 0.41 ± 0.02 SD in non-pockmarks) (Fig. 3). Overall, crenarchaeol and GDGT-0 together account for ~96 % in both sediment types, with similar proportions in the two settings. In this dataset, GDGT-0 covaries very tightly with crenarchaeol (Pearson $r = 0.996$, n = 72, BH–FDR $q = 2.03 \times 10^{-75}$; pearma ρ = 0.983, BH–FDR $q = 2.06 \times 10^{-52}$).

https://doi.org/10.5194/egusphere-2026-519
Preprint. Discussion started: 4 February 2026


The remaining iGDGTs (GDGT-1 to GDGT-3) occur only in minor proportions and at much lower concentrations. Spatially, the highest ΣiGDGT concentrations occur at sites in the Gdańsk Deep (MET3, MET4), whereas the relative dominance of crenarchaeol and GDGT-0 remains similar between pockmark and non-pockmark sediments across the study area. All concentration profiles of individual iGDGTs (supplementary material Fig. S1) follow very similar patterns (with outliers in MET1-BH/6 and MET4/3), except for minor changes in the crenarchaeol isomer (cren′) at MET1-MP and MET1-BH, and even smaller differences at MET3 and MET4. GDGT-1, GDGT-2, and GDGT-3 also covary strongly with crenarchaeol (Pearson $r$ = 0.988, 0.954, 0.951; Spearman ρ = 0.961, 0.915, 0.937; all BH–FDR $q < 0.05$; n = 72). Across all iGDGT pairs, correlations are consistently strong (Pearson $r$ = 0.847–0.996, all BH–FDR $q \leq 6.43 \times 10^{-21}$; Spearman ρ = 0.685–0.986, all BH–FDR $q \leq 3.16 \times 10^{-11}$; n = 72). The GDGT-0/crenarchaeol ratio varies between 0.65 and 0.99 in pockmark sediments and between 0.63 and 0.91 in non-pockmark sediments. Overall, these ratios show no consistent depth trend across all cores; when changes occur, they are site-specific and modest compared with the overlap between pockmark and non-pockmark sediments.

In all cores, GDGT-0/cren ratios are moderate and generally comparable across sediment types, ranging from 0.65 to 0.99 in pockmarks and from 0.63 to 0.91 in non-pockmark sediments. The GDGT-2/cren ratio is consistently low (0.01–0.04). In line with this, Methane Index (MI) values show no clear distinction and remain low throughout the profiles. MI exhibits little variability in pockmark sediments (0.04–0.09) and in non-pockmark sediments (0.03–0.07), indicating similarly low values in both settings.

https://doi.org/10.5194/egusphere-2026-519
Preprint. Discussion started: 4 February 2026


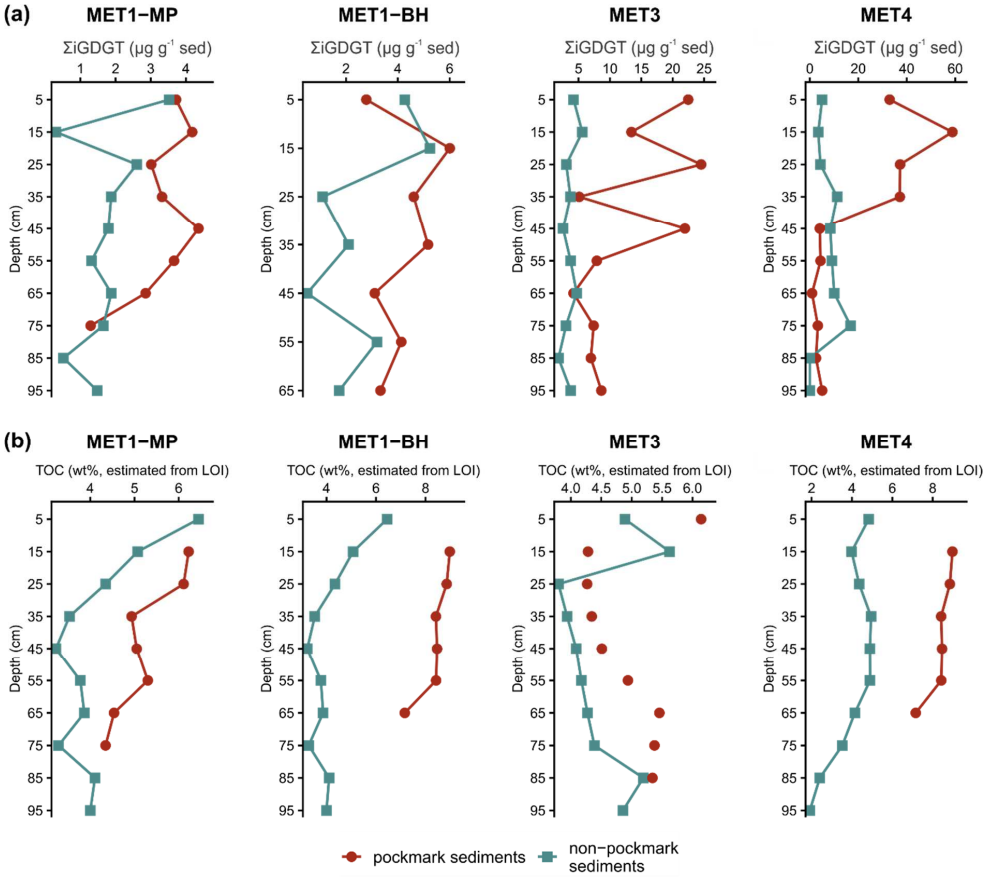


Fig. 2. Downcore profiles of (top row; (a) summed isoprenoidal glycerol dibiphytanyl glycerol tetraethers (ΣiGDGTs; µg g⁻¹ dry sediment) and (bottom row; (b) total organic carbon (TOC; wt %, estimated from LOI) for sediment cores from four sites in the south-eastern Baltic Sea: MET1-MP and MET1-BH (Gulf of Gdańsk), and MET3 and MET4 (Gdańsk Deep). In (a), concentrations are plotted as a function of depth (cm), showing a general downcore decrease. Note that x-axis scales vary among panels. ΣiGDGTs exhibit elevated concentrations in pockmark sediments relative to adjacent reference sediments, with the most pronounced enrichments observed at the Gdańsk Deep sites (MET3, MET4), where elevated near-surface values are followed by a marked downcore decrease. In (b), TOC values were estimated from LOI using the Bay of Gdańsk LOI–TOC calibration (Łukawska-Matuszewska et al., 2014) and are presented for qualitative comparison of downcore trends (validation in supplementary material Fig. S1, S2). TOC concentrations are consistently elevated in pockmark sediments — most notably at MET4 — broadly paralleling the enhanced ΣiGDGT abundances.

Table 1. Mean GDGT-based indices for pockmark (P) and reference (S) sediment cores at MET1 (MP, BH), MET3, and MET4. Metrics include OH-GDGT%, hydroxylated GDGT ring indices (RI-OH, RI-OH′), Methane Index (MI), and diagnostic ratios (GDGT-0/cren, GDGT-2/cren). RI-OH exhibits minimal variation among sites and sediment types (≈1.1–1.2), indicating comparable OH-GDGT cyclization patterns. OH-GDGT% is moderately elevated at MET1 relative to MET3–MET4, with minimal within-site differences. MI values remain consistently low (0.05–0.07), indicating weak

https://doi.org/10.5194/egusphere-2026-519
Preprint. Discussion started: 4 February 2026


methanotrophic influence on bulk GDGT distributions. GDGT-0/cren ratios are consistently elevated in pockmark cores relative to paired references, whereas GDGT-2/cren remains uniformly low (0.01–0.02), indicating that pockmark influence primarily affects GDGT-0 abundance rather than higher-cyclized GDGTs.

| Sediment core | OH-GDGT% | RI-OH | RI-OH' | MI | GDGT-0/cren | GDGT-2/cren |
|---|---|---|---|---|---|---|
| **P/MET1-MP** | 9.0 | 1.2 | 0.19 | 0.07 | 0.84 | 0.02 |
| **P/MET1-BH** | 9.3 | 1.2 | 0.19 | 0.07 | 0.92 | 0.02 |
| **P/MET3** | 7.9 | 1.2 | 0.21 | 0.07 | 0.76 | 0.02 |
| **P/MET4** | 7.8 | 1.1 | 0.19 | 0.05 | 0.74 | 0.01 |
| **S/MET1-MP** | 8.1 | 1.2 | 0.25 | 0.07 | 0.79 | 0.02 |
| **S/MET1-BH** | 8.1 | 1.2 | 0.23 | 0.07 | 0.80 | 0.02 |
| **S/MET3** | 7.0 | 1.2 | 0.19 | 0.05 | 0.73 | 0.01 |
| **S/MET4** | 7.2 | 1.2 | 0.21 | 0.07 | 0.69 | 0.02 |

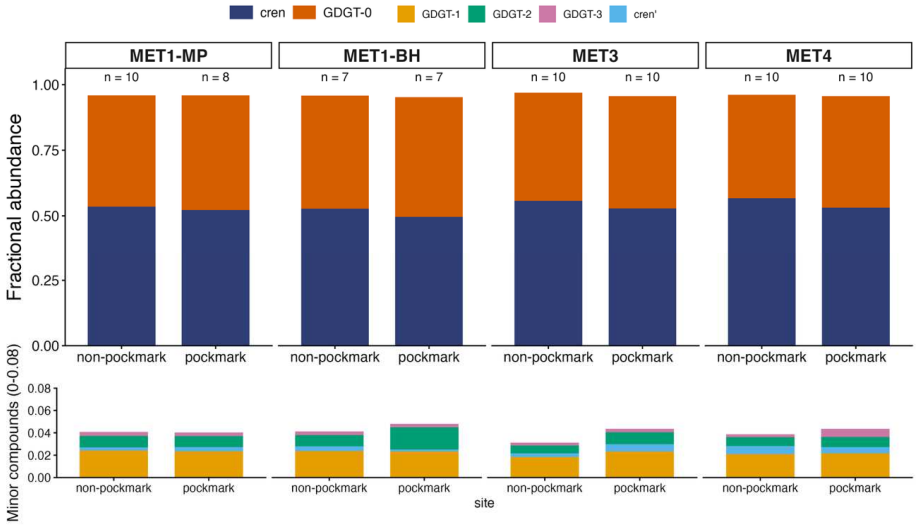


Fig. 3. Mean iGDGT fractional abundances in pockmark and non-pockmark sediments at four sites in the south-eastern Baltic Sea. Stacked bars represent mean fractional abundances of iGDGTs (GDGT-0–3, crenarchaeol, and cren′), averaged by site and sediment type; *n* indicates the number of horizons (samples). The upper panel shows the full scale (0–1), whereas the lower panel expands the y-axis (0–0.08) to resolve minor constituents. Crenarchaeol and GDGT-0 dominate across all sites, whereas GDGT-1–3 and cren′ constitute minor fractions with greater variability. Compositional differences between pockmark and non-pockmark sediments are subtle and are primarily manifested in minor components (e.g. elevated GDGT-2 and/or cren′ in certain pockmark settings).

### 3.3 OH-GDGTs in pockmark and non-pockmark sediments

The abundance and distribution of hydroxylated GDGTs (OH-GDGT-0 to -2) in pockmark sediments and in surrounding non-pockmark reference sediments broadly reflect those of iGDGTs, with uniformly positive and very strong cross-correlations (Pearson $r$ = 0.840–0.992

https://doi.org/10.5194/egusphere-2026-519
Preprint. Discussion started: 4 February 2026


and Spearman ρ = 0.602–0.975) and the tightest coupling with GDGT-0 (ΣOH-GDGTs: Pearson $r = 0.992$, $q = 4.44 \times 10^{-64}$; □pearma□ρ = 0.975, $q = 2.51 \times 10^{-46}$) and crenarchaeol (Pearson $r = 0.983$, $q = 3.74 \times 10^{-53}$; Spearman ρ = 0.935, $q = 5.15 \times 10^{-33}$). All targeted OH-GDGTs were detected in both settings.

Summed OH-GDGT concentrations (ΣOH-GDGTs) span 0.00–6.30 μg $g^{-1}$ sediment across all samples (Fig. 4), with values generally higher in pockmarks (0.06–6.30 μg $g^{-1}$ sediment; median 0.43 μg $g^{-1}$ sediment; mean 1.02 μg $g^{-1}$ sediment) than in non-pockmark sediments (0.00–1.75 μg $g^{-1}$ sediment; median 0.21 μg $g^{-1}$ sediment; mean 0.31 μg $g^{-1}$ sediment). ΣOH-GDGTs are on average approximately three times higher and about two times higher at the median in pockmarks relative to non-pockmarks. Spatially, the highest ΣOH-GDGTs occur at MET4, intermediate values at MET3, and the lowest in the MET1 area, mirroring the northward increase observed for ΣiGDGTs. With depth, ΣOH-GDGTs commonly show shallow to mid-depth maxima (typically 15–45 cm), followed by downcore depletion that varies among cores, with concentrations typically decreasing by a factor of ~2.8 in MET1–MET3 but reaching ~102 in MET4 (e.g. from 6.30 to 0.06 μg $g^{-1}$ sediment in P/MET4) and approaching zero in the deepest non-pockmark reference horizons of S/MET4.

Across all cores, OH-GDGTs are dominated by OH-GDGT-0 in both pockmark and non-pockmark sediments (FA = 0.83 ± 0.02 SD and 0.82 ± 0.03 SD, respectively), whereas OH-GDGT-1 and OH-GDGT-2 are consistently minor components (Fig. 5). The OH-GDGT distributions are broadly similar between the two sediment types (supplementary material Fig. S4) Most variability is expressed in downcore concentration profiles, which typically decline by a factor of ~1.2 to ~7.8, with most cores showing a decrease by a factor of ~3 (P/MET1-BH ends higher at the bottom, whereas S/MET4 peaks mid-core and declines to zero at the base). Across all OH-GDGT pairs (OH-0, OH-1, OH-2), correlations are consistently very strong (Pearson $r = 0.975$–$0.992$, all BH-FDR $q \leq 1.60 \times 10^{-49}$, $n = 75$; Spearman ρ = 0.922–0.974, all BH-FDR $q \leq 7.18 \times 10^{-32}$, $n = 75$).

OH-GDGT% and RI-OH show only minor differences between sediment types (Table 1). OH-GDGT% values in pockmarks are only slightly higher (6.4–9.9; mean 8.4 ± 1.1 SD) than in non-pockmark sediments (6.2–9.4; mean 7.6 ± 0.9 SD). RI-OH is nearly identical between settings (1.18 ± 0.04 SD in pockmarks; 1.19 ± 0.04 SD in non-pockmarks), whereas RI-OH′ is modestly higher in non-pockmark sediments (0.22 ± 0.05 SD) than in pockmarks (0.20 ± 0.02 SD). Overall, variability is more pronounced between cores than between pockmark and non-pockmark sediments. Thus, variability in OH-GDGTs is mainly expressed in absolute concentrations, with methane-rich pockmarks, particularly P/MET4, showing the highest enrichment. The composition of OH-GDGTs and associated indices exhibits broadly similar characteristics in both pockmark and non-pockmark sediments.

https://doi.org/10.5194/egusphere-2026-519
Preprint. Discussion started: 4 February 2026


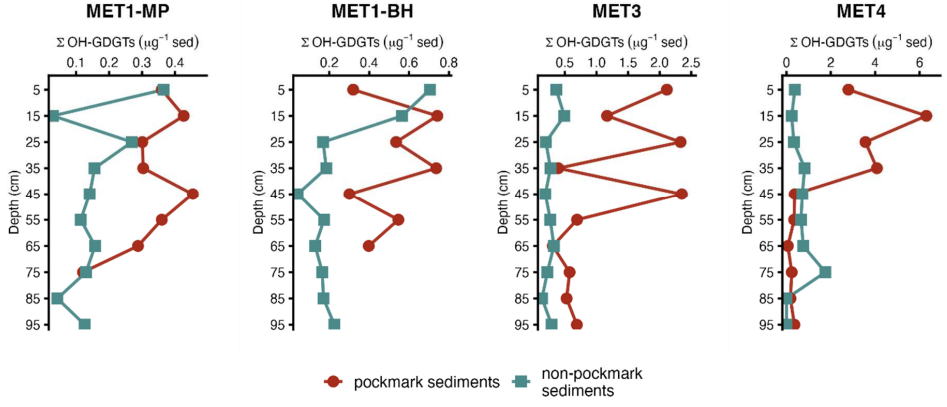


Fig. 4. Downcore profiles of summed hydroxylated glycerol dibiphytanyl glycerol tetraethers (ΣOH-GDGTs; μg $g^{-1}$ dry sediment) for sediment cores from four sites in the south-eastern Baltic Sea: MET1-MP and MET1-BH (Gulf of Gdańsk) and MET3 and MET4 (Gdańsk Deep). Concentrations are plotted as a function of depth (downcore increase; cm). ΣOH-GDGT concentrations follow the pattern of iGDGTs, with strong positive cross-correlations and the highest coupling with GDGT-0 and crenarchaeol (see Section 3.2). In the Gulf of Gdańsk (MET1-MP, MET1-BH), ΣOH-GDGTs display lower overall abundances than iGDGTs yet remain elevated in pockmark intervals relative to reference sediments.

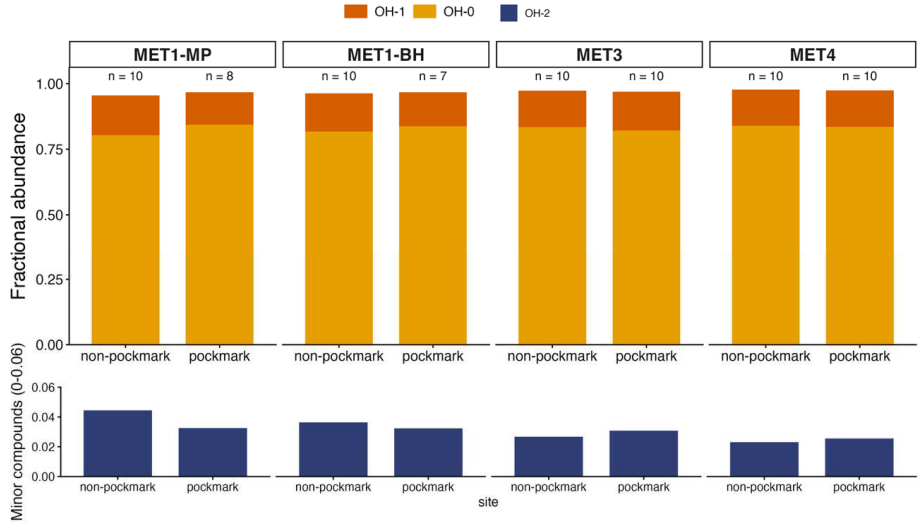


Fig. 5. Mean OH-GDGT fractional abundances in pockmark versus non-pockmark sediments at four sites in the south-eastern Baltic Sea. Stacked bars represent mean fractional abundances of OH-0, OH-1 and OH-2, averaged by site and sediment type; *n* denotes the number of horizons (samples). The upper panel presents the full scale (0–1), whereas the lower panel expands the y-axis (0–0.06) to resolve OH-2. OH-0 dominates across all sites, with OH-1 contributing a smaller yet consistent fraction and OH-2 occurring at low abundance. Compositional differences between pockmark and non-pockmark sediments are modest, primarily manifested in OH-2, which exhibits slight variability among sites.

https://doi.org/10.5194/egusphere-2026-519
Preprint. Discussion started: 4 February 2026


### 3.4 Abundance and composition of archaea

Pockmark and reference sediments in the Baltic Sea display markedly different archaeal community structures (Fig. 6a). Nearly all samples are dominated by Nanoarchaeia and Thermoplasmata, with additional contributions from Methanosarcinia (P/MET1-MP, P/MET4) and Bathyarchaeia (S/MET3, S/MET4). Archaeal abundances are consistently higher in pockmarks, particularly at MET3 and MET4, where populations peak at shallow to mid-depths (5–45 cm). Reference sediments (non-pockmarks), in contrast, show lower overall archaeal abundance but greater taxonomic diversity, with elevated proportions of Thermoplasmata, Bathyarchaeia, Lokiarchaeia and Nitrososphaeria (Fig. 6). Methanogenic archaea (Methanosarcinia, Methanobacteria, Methanomicrobia) and AOM-related taxa (ANME-2b) are more common in pockmarks (supplementary material, Fig. S6–S8), while Nanoarchaeia, although dominant in both settings – particularly the genus *AR15* – are proportionally enriched in pockmarks (Fig. 6a).

Methanogen community composition varies with depth, with *Methanosarcina* and *Methanosaeta* typically dominating, especially in non-pockmark reference sediments (Supplementary Material Fig. S7). *Candidatus Nitrosopumilus* (Nitrososphaeria) is notably enriched in reference sediments, where this ammonia-oxidising archaeon (AOA) can account for up to 70% of the community (Supplementary Material Fig. S6). Conversely, methane-cycling archaea – particularly Methanosarcinia – dominate pockmarks, constituting up to ~30% of the total archaeal population (P/MET4), especially at greater depths (Fig. 6a). This pattern is most pronounced in MET4, where ANME-2b reaches ~40% and dominates the lower sediment profile (supplementary material Fig. S6b), while methanotrophic taxa are largely absent from reference cores (supplementary material Fig. S8).

Thermoplasmata, Bathyarchaeia and Lokiarchaeia show contrasting distributions between sediment types. Thermoplasmata reaches up to 11% in pockmarks but is more prevalent in reference cores, reaching ~30% in MET1-BH (Fig. 6a). Bathyarchaeia is particularly abundant in reference sediments, peaking at 70% at 45 cm depth in MET4, compared with <7% in pockmarks (Fig. 6a). Lokiarchaeia follows a similar pattern, constituting ~6% in references versus ~3% in pockmarks (Fig. 6a).

Other archaeal groups – including Thermococci, the Deep Sea Euryarchaeotic Group (DSEG), Methanomicrobia and Iainarchaeia – show greater variability, contributing up to 5% across both sediment types (Fig. 6a). Some taxa are habitat-specific: Methanobacteria and Methanonatronarchaeia occur mostly in pockmarks, whereas ANME-1 and Heimdallarchaeia are found chiefly in reference cores, although all are present at low abundances (Fig. 6a, b).

Depth-dependent patterns further distinguish the two sediment types. In pockmarks, archaeal abundances typically peak at mid-depths (40–45 cm), with the highest value (~30,000 reads) in the upper horizon of P/MET4 (supplementary material Fig. S9). Reference sediments show lower overall abundances (maximum ~18,000 reads), with flatter depth profiles and increasing proportions of Bathyarchaeia and Thermoplasmata with depth.

Hierarchical clustering of relative abundances reveals four distinct groups (Fig. 6b): Cluster 1 comprises pockmark samples; Cluster 2 combines reference and pockmark samples; Cluster 3 consists mainly of reference samples; and Cluster 4 includes two reference samples surrounding MET1-BH plus the P/MET4-10 sample (outliers).

https://doi.org/10.5194/egusphere-2026-519
Preprint. Discussion started: 4 February 2026


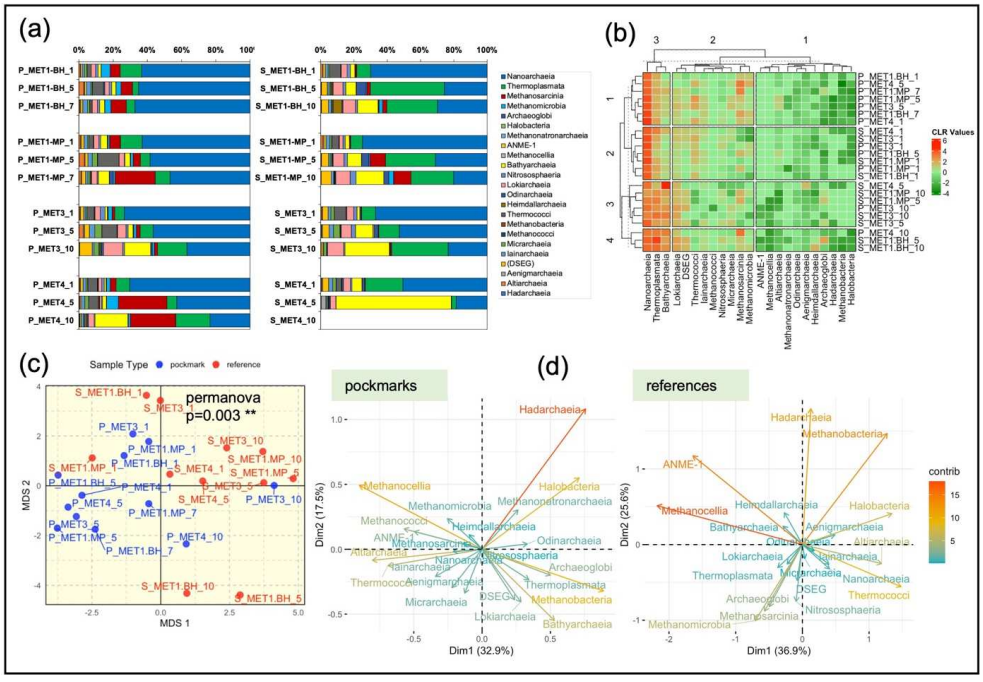


Fig. 6. Archaeal community composition and multivariate structure in pockmark versus reference sediments from four sites. (a) Relative abundance profiles (stacked bars) of archaeal taxonomic groups, shown separately for pockmark (P) and reference (S) sediments. (b) Heatmap of CLR-transformed community data showing covariation among taxa and samples; dendrograms show hierarchical clustering. Colour intensity reflects centred log-ratio (CLR)-transformed relative abundances, where red represents higher relative enrichment and green indicates lower relative enrichment. (c) NMDS ordination showing separation between pockmark (blue) and reference (red) samples (PERMANOVA, p = 0.003). (d) Ordination biplots for pockmarks and references, showing taxa contributing most to within-group variability. Nanoarchaeia dominate across all sites. Pockmark horizons show elevated Methanosarcinia (MET1-MP, MET4), whereas reference horizons show stronger Thermoplasmata and/or Bathyarchaeia contributions. Hierarchical clustering reveals partial intermixing of pockmark and reference samples, indicating that community structure reflects both habitat type and site-specific variability. NMDS shows significant separation (PERMANOVA, $p$ = 0.003), with reference samples more dispersed and pockmark samples more tightly grouped. Taxa driving within-group variability differ between habitats: Hadarchaeia and Halobacteria dominate the pockmark ordination, whereas Methanobacteria, ANME and Hadarchaeia drive the reference ordination.

The differences between pockmark and reference samples appear to be statistically significant. Multivariate analysis based on MDS demonstrates the clustering of samples into two distinct categories: pockmarks versus reference sediments (Fig. 6c). The PERMANOVA test confirmed the statistical significance of these differences at $p$ = 0.003. However, some variation is evident — pockmark samples are more tightly clustered, whereas reference samples appear slightly more dispersed. Based on these analyses, it can be inferred that methane-bearing sediments (pockmarks) differ significantly in their archaeal composition from the surrounding, non-pockmark sediments, here defined as reference samples. PCA further identified the groups

https://doi.org/10.5194/egusphere-2026-519
Preprint. Discussion started: 4 February 2026


contributing most to the differentiation of samples (Fig. 6d). In the case of pockmarks, the groups with the greatest influence on sample variability are Hadarchaeia > Methanobacteria > Methanocellia > Halobacteria. In reference samples, the key contributors are Methanocellia > ANME-1 > Methanobacteria > Hadarchaeia. While the same groups largely explain the variability in both cases, the proportions of their contributions differ, resulting in distinct community compositions, as confirmed by previous analyses.

### 3.5 Correlation network

To link GDGT patterns to probable biological sources, we combined iGDGT and OH-GDGT abundances with archaeal 16S rRNA (family-level) relative abundances using correlation network analysis. This approach identified co-varrying lipid – taxon modules that may indicate common sources, ecological niches, or interconnected processes rather than direct biosynthesis alone.

In pockmark sediments, the correlation network resolves three main co-varying archaeal communities (Fig. 7). The first community (red) comprises the full suite of measured GDGTs and is most strongly connected to several Nanoarchaeia lineages (GW2011, SCGC_AAA286_E23, CG1.02.57.44, SCGC_AAA011.D5), with additional links to *Methanoperedenaceae*. The second community is dominated by ammonia-oxidising *Nitrosopumilaceae* and clusters with Hadarcheales. Within this module, *Nitrosopumilaceae* show the strongest positive links to GDGT-0 and the remaining iGDGTs along with OH-GDGTs. The same module contains ANME-2a/2b, *Methanoregulaceae*, and uncultured lineages that are strongly interconnected with one another but show comparatively weaker links to GDGTs. *Archaeoglobaceae* forms a peripheral node and does not meet the edge-retention criteria with any GDGTs in pockmarks. The third community groups methanogenic lineages, including *Methanospirillaceae, Methanobacteriaceae, Methanosarcinaceae, Methanosaetaceae, Methanomicrobiaceae, Methanomassiliicoccaceae* and CG1.02.32.21 (associated with the order *Micrarchaeales*). These are less directly connected to GDGTs but strongly interlinked with one another. This cluster also contains another Nanoarchaeia representative (GW2011_GWC1_47_15).

In reference sediments, GDGT associations are distributed more broadly across archaeal groups, and the network exhibits higher modularity, with clearer separation among modules. A lipid cluster (crenarchaeol, cren', GDGT-0-3, and OH-GDGTs) correlates with both ammonia oxidisers (*Nitrosopumilaceae, Nitrososphaeraceae*) and multiple methanogenic families (*Methanosaetaceae, Methanosarcinaceae, Methanoregulaceae, Methanomicrobiaceae, Methanomassiliicoccaceae*). Compared with pockmarks, methanogens show fewer direct links to the GDGT cluster and more to ANME-2a/2b. *Archaeoglobaceae* remains peripheral but shows weak links to *Nitrososphaeraceae* and methanogens.

Overall, the pockmark network shows low modularity and relatively dense connectivity, indicating a closely coupled archaeal community. At the same time, the strongest GDGT links centre on *Nitrosopumilaceae*, implying that AOA dominate GDGT co-variation in these methane-rich sediments, while methanogens/ANME form more distinct subclusters with weaker GDGT coupling.

https://doi.org/10.5194/egusphere-2026-519
Preprint. Discussion started: 4 February 2026


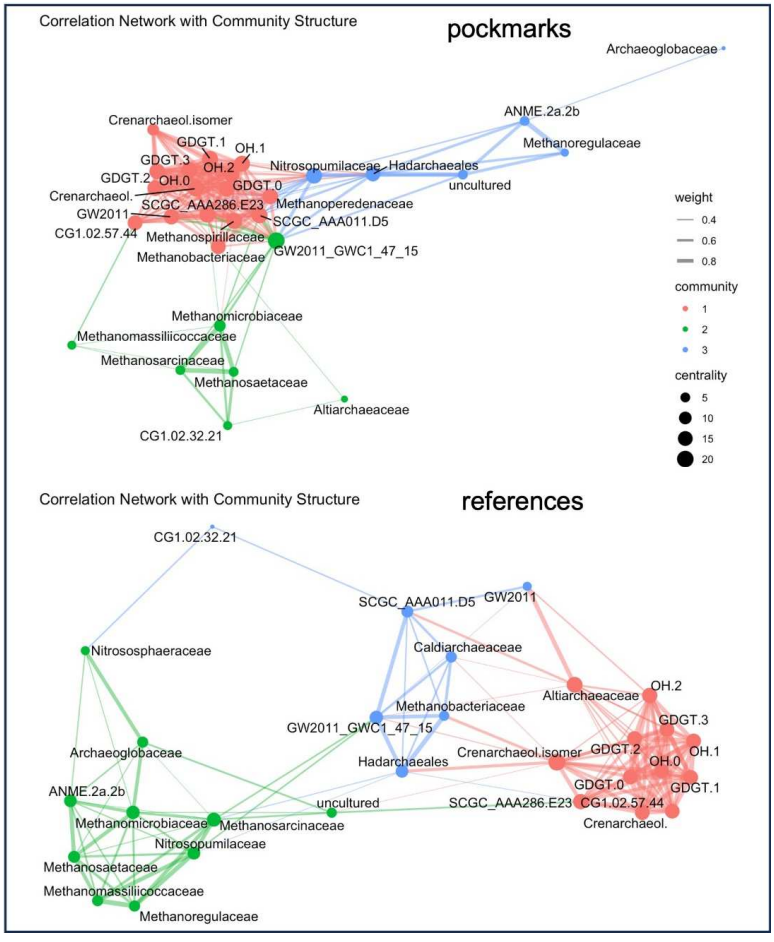


Fig. 7. Correlation networks linking archaeal lipid biomarkers and community members in pockmark and reference (non-pockmark) sediments. Nodes represent lipid variables (GDGTs, OH-GDGTs) and archaeal taxa (family level). Edge thickness reflects correlation strength; node colour denotes modules/communities (1–3); node size reflects centrality (larger nodes indicate more central or highly connected features). Lipid variables form a tightly connected subnetwork (module 1; red), while additional modules comprise methane-cycling and other archaeal lineages. Module connectivity differs between sediment types, indicating habitat-dependent coupling between biomarkers and archaeal taxa. Pockmark networks show tighter coupling between lipid biomarkers and methane-cycling lineages, whereas reference sediments display clearer module separation, with lipids and the archaeal community varying more independently.

## 4 Discussion

### 4.1 Archaeal community diversity and methanogenesis

Pockmark sediments exhibit substantially higher methanogen diversity (11 genera detected) and a higher abundance of methane-cycling archaea (approximately threefold) compared with non-pockmark reference sediments (six genera). Correspondingly, total iGDGT and OH-GDGT

https://doi.org/10.5194/egusphere-2026-519
Preprint. Discussion started: 4 February 2026


concentrations are approximately three times higher in pockmarks than in non-pockmark references. In the correlation network (Fig. 7), pockmarks represent a tightly coupled metabolic system in which various archaeal groups act in concert — likely carrying out methanogenesis and ammonia oxidation — whereas at the reference (non-pockmark) sites these groups form less integrated sub-communities. This suggests that, in the absence of fluid seepage, these microorganisms adopt more independent or niche-partitioned ecological roles.

*Methanosarcina* predominates throughout all sediment horizons in both pockmark and non-pockmark reference sediments, likely owing to its metabolic versatility (Sowers et al., 1993; Galagan et al., 2002; Maeder et al., 2006), which confers competitive advantages under fluctuating environmental conditions (e.g., hydrostatic pressure governing seeps, seasonal thermocline dynamics, nutrients availability, North Sea saline water inflow). The vertical distribution of methanogenic archaea shifts with sediment depth, with *Methanosarcina* and *Methanosaeta* predominating, particularly in non-pockmark reference sediments. Both taxa drive acetoclastic methanogenesis (Conklin et al., 2006; Welte et al., 2014) and are favoured in sediments with high labile organic matter (Li et al., 2022). In MET1-MP and MET1-BH sites, their abundance remains high, consistent with elevated TOC LOI-based levels (**Error! Reference source not found.**b). Both are major contributors to the GDGT-0 pool in estuarine sediments (De Rosa et al., 1977; Schouten et al., 2013; Bauersachs et al., 2015). GDGT-0 is the second most abundant GDGT in the analysed samples (**Error! Reference source not found.**) and exhibits fluctuating concentrations in the MET1-area pockmarks (supplementary material Fig. S1), which are characterised by strong SGD.

In contrast, *Methanosaeta* abundance declines sharply with depth in MET3 and MET4 and is replaced by diverse hydrogenotrophic genera, including *Methanospirillum, Methanogenium*, *Methanomicrobium, Methanoculleus, Methanocorpusculum, Methanobrevibacter,* and *Methanolinea*. MET4 pockmark sediments, characterised by the highest total GDGT concentrations and the most pronounced individual GDGT peaks (Fig. 2, 4; supplementary material Fig. S1), harbour exceptionally abundant hydrogenotrophic methanogens (particularly *Methanoregula*) alongside *Methanosarcina*, with the MET3 pockmark showing the next highest abundance. These hydrogenotrophs belong to the class Methanomicrobia and are known to produce acyclic GDGTs (Bale et al., 2019; Zeng et al., 2022), with a genus like *Methanobrevibacter* identified as a GDGT-0 producer (Bauersachs et al., 2015; Elling et al., 2017). Similar hydrogenotrophic communities have been documented in an inactive pockmark in the Hanko Basin, northern Baltic Sea (Purkamo et al., 2022). In this dataset, pockmark MET3 was also inactive during the study period, and pockmark MET4 is characterised by low-intensity SGD.

Pronounced differences are observed among sites. *Methanoregula* is notably absent from MET3 sediments. Contrary to earlier observations suggesting a near-absence of methanogens at MET3 (Brodecka-Goluch et al., 2022), the 16S rRNA gene data reveal multiple methanogenic lineages (as noted above) throughout the sediment profile, indicating episodic or niche-specific methanogenic activity. MET4 hosts the most diverse and abundant methanogen community (supplementary material Fig. S9), coinciding with exceptionally high GDGT concentrations (**Error! Reference source not found.**, 4), which suggests efficient production and favourable preservation of GDGTs. Elevated GDGT concentrations in MET4 and MET3 may reflect deposition in a fine-grained depocenter of the Gdańsk Basin/Gdańsk Deep, where sediment focusing (including trapping within the concave pockmark morphology) and accumulation can be substantial, although the Gulf of Gdańsk also exhibits high accumulation driven by terrigenous input. However, the MET3 and MET4 study sites were characterised by

https://doi.org/10.5194/egusphere-2026-519
Preprint. Discussion started: 4 February 2026


stable, non-ebullitive methane emissions, which could have contributed to the better preservation of iGDGTs.

Several archaeal groups, including Thermoplasmata, Bathyarchaeia, Lokiarchaeia, Heimdallarchaeia, Archaeoglobi, and the Deep Sea Euryarchaeotic Group (DSEG), are associated with the degradation of complex organic matter, aromatic carbon breakdown, protein catabolism, and fermentation (Zinke et al., 2019). These groups — particularly Bathyarchaeia and Thermoplasmata — are more abundant in non-pockmark sediments than in pockmarks and may contribute to GDGT production in anoxic environments (Besseling et al., 2018, 2020; Baxter et al., 2021). Bathyarchaeia thrive in anoxic settings, degrading recalcitrant organic matter (Baxter and Zalar, 2019; Blewett et al., 2022; Zeng et al., 2022), while Archaeoglobi mediate both sulphate reduction and methanogenesis (Lynes et al., 2024). Asgard archaea, including hydrocarbon-degrading Lokiarchaeia and hydrogen-dependent acetogenic Heimdallarchaeia (Zhang et al., 2025), also show higher abundance in non-pockmark sediments and may contribute to iGDGT production, likely GDGT-0 (Zeng et al., 2022). Although the tetraether synthase (tes) gene, essential for GDGT biosynthesis, has been identified in Hadarchaeia and Altiarchaeia, GDGTs have not yet been detected in these groups (Zeng et al., 2022). Notably, some Hadarchaeia grow syntrophically with methanogens (Yu et al., 2024).

Pockmark sediments exhibit more frequent shifts in the dominance of alternative methanogenic genera than non-pockmark sediments, which may reflect the dynamic geochemical conditions characteristic of these gas systems.

### 4.2 Assessing AOM: iGDGT indices and ANME composition

Peaks in archaeal abundance and GDGT concentrations within 5–45 cm sediment depth may mark the sulphate–methane transition zone (SMTZ), strongest at MET4 and MET3 and weakest at MET1 (Fig. 2). This pattern inversely correlates with gas flow and bubbling intensity reported previously (Jaśniewicz et al., 2019; Brodecka et al., 2013; Idczak et al., 2020; Brodecka-Goluch et al., 2022; Kurowski et al., 2024). However, iGDGTs indices (Table ) do not support a strong AOM imprint, as values remain uniformly low. MI values (<0.09) fall well below the 0.3-0.5 threshold indicative of methane-impacted sediments observed by Zhang et al. (2011).

The MI index, calculated as the ratio of GDGT-1-3 to crenarchaeol, typically indicates minimal methanotrophic contribution relative to Nitrososphaeria-derived sources when low (Zhang et al., 2011). The uniformly low MI values observed here likely reflect a strong crenarchaeol signal from ammonia-oxidising archaea (Fig. 3) and/or limited GDGT-1-3 production by the dominant AOM lineages, rather than definitively excluding AOM. GDGT-1 to -3, which increase substantially in ANME-1-dominated systems (Rossel et al., 2008), are two orders of magnitude less abundant in the analysed samples, consistent with the near-absence of ANME-1 (maximum relative abundance of 0.6% in S/MET3/5; Fig. 6). Correspondingly, only the inactive pockmark MET3 exhibited relatively elevated sulphate concentrations among the sites previously examined (Brodecka-Goluch et al., 2022).

Although the applicability of MI to ANME-2 and ANME-3 (which dominate the AOM community here; supplementary material Fig. S8, S9) has been questioned, comprehensive biomarker investigations generally validate its utility for AOM detection (Kim and Zhang, 2023). Nevertheless, ANME-2 and ANME-3 alone are unlikely to contribute substantially to GDGT production (Niemann and Elvert, 2008; Weijers et al., 2011), rendering MI non-diagnostic in the analysed settings. The consistently low GDGT-2/cren ratios (maximum 0.4)

https://doi.org/10.5194/egusphere-2026-519
Preprint. Discussion started: 4 February 2026


corroborate this interpretation. This ratio typically indicates methane-rich AOM conditions when ANME-1-synthesized GDGT-2 (Rossel et al., 2008) is elevated relative to crenarchaeol.

Nevertheless, ANME lineages are more prevalent in pockmark sediments (supplementary material Fig. S6, S8), suggesting enhanced AOM activity, particularly at MET3 and MET4. Peaks in GDGT-1 to -3 concentration also occur at non-pockmark reference sites, though at lower concentrations, following the general trend for all iGDGTs (supplementary material Fig. S3). The limited contribution of GDGT-1-3 to bulk GDGTs likely reflects the low sulphate concentrations documented previously (Brocławik et al., 2020; Brodecka-Goluch et al., 2022; Idczak et al., 2020; Łukawska-Matuszewska et al., 2022; Ehlert von Ahn et al., 2024), which constrains the metabolic activity of sulphate-dependent ANME clades (Timmers et al., 2015). In addition, certain core GDGTs (e.g., GDGT-1) may originate from diagenesis and degradation of phosphohexose headgroups predominantly produced by *Nitrosopumilus* in the Baltic Sea (Wittenborn et al., 2023).

Overall, AOM activity appears constrained in studied pockmarks, consistent with previous investigations demonstrating weak AOM confined to thin, shallow sediment layers and potentially dependent on alternative electron acceptors (Brocławik et al., 2020; Idczak et al., 2020; Brodecka-Goluch et al., 2022; Łukawska-Matuszewska et al., 2022; Ehlert von Ahn et al., 2024). The minor contribution of *Ca. Methanoperedens* in the dataset (MET1-MP; supplementary material Fig. S8) further supports AOM coupled to nitrate and/or metal oxide reduction. Members of the family *Methanoperedenaceae* (formerly ANME-2D) typically inhabit sulphate-depleted freshwater systems and conduct AOM independently of syntrophic partnerships (Haroon et al., 2013; Ettwig et al., 2016; Vaksmaa et al., 2017; Leu et al., 2020).

Within the methane-cycling archaeal community, methanogens appear to be the principal contributors to GDGT biosynthesis (Fig. 7). Although GDGT-0 and crenarchaeol predominate in marine sediments (Schouten et al., 2002), their elevated concentrations across all investigated gas systems indicate that they function as primary iGDGTs biomarkers in the sediments of the Gdańsk Basin, even in methane-rich settings harbouring both methanogenic and methanotrophic communities. However, GDGT-0 lacks source specificity and can be synthesised by multiple archaeal lineages, including methanogens and methanotrophs (Pancost et al., 2001; Blaga et al., 2009; Inglis et al., 2015; Słowakiewicz et al., 2016; Petrick et al., 2019), which may also produce cyclised GDGTs (Koga et al., 1993; Weijers et al., 2006; Schouten et al., 2013; Bauersachs et al., 2015), although this is not always replicable in culture studies (Bauersachs et al., 2015).

### 4.3 AOA-driven GDGT signatures in pockmarks: the dominance of crenarchaeol

The network analysis indicates that AOA-associated lipids (crenarchaeol and statistically co-varying GDGT-0) are the primary drivers of variation in the bulk GDGT pool (Fig. 7), likely masking the methanogen signal through the influence of Nitrososphaerota on the GDGT-0/cren ratio. The observed GDGT-0/cren ratios below 0.99 in Gdańsk Basin samples fall well below the threshold of 2, characteristic of methanogen-dominated systems (Schouten et al., 2002; Blaga et al., 2009), indicating minimal methanogen contribution and AOA predominance. Despite this AOA dominance, GDGT-0 concentrations remain relatively elevated across the pockmark sites, particularly at the inactive pockmark P/MET3 and the low-SGD pockmark MET4, compared with active venting systems characterised by advective methane flow, such as mud volcanoes on the Canadian Beaufort Sea slope (Lee et al., 2018).

https://doi.org/10.5194/egusphere-2026-519
Preprint. Discussion started: 4 February 2026


Methane seepage creates chemically reducing conditions that limit the growth of oxygen-requiring organisms. However, seep systems also generate sharp chemical gradients and microenvironments (e.g., thin oxic/suboxic boundary layers) in which AOA can survive and function (Jakobs et al., 2016). Consequently, crenarchaeol remains the dominant iGDGT in both pockmark and reference sediments (Fig. 3), as it is abundant in the overlying water column.

In the northern Baltic Sea pockmarks (Hanko Basin), Nitrososphaeria – including some populations of groundwater origin – constitute a major component of the archaeal community (Purkamo et al., 2022), consistent with evidence that *Ca. Nitrosopumilus* is widespread in the Baltic Sea and represents an important GDGT-producing lineage (Wittenborn et al., 2023). However, amplicon-based relative abundance reflects the compositional distribution of recovered 16S rRNA gene reads after DNA extraction (Gloor et al., 2017), rather than directly measuring lipid production rates, whereas sedimentary iGDGTs integrate archaeal lipid production and export over longer timescales, with their distribution further shaped by preservation conditions (Lengger et al., 2013). Given that AOA are abundant in the Baltic Sea under low-oxygen conditions and along redox gradients (Berg et al., 2015b), the consistently low GDGT-0/cren ratios (<1) observed herein indicate a crenarchaeol-rich iGDGT pool, suggesting substantial pelagic contribution from the settling and export of AOA-derived crenarchaeol from the water column.

Nanoarchaeota, prevalent across the samples, are likely involved in ectosymbiosis with Nitrososphaeria, consistent with their reliance on symbiotic relationships (Waters et al., 2003). Nanoarchaeota may also possess GDGTs, previously attributed to their biological hosts (Zeng et al., 2022), which could explain their correlation with GDGTs (Fig. 6). They can also associate with methanogens (Brick et al., 2025), which may account for their high relative abundance (~40% in non-pockmark and ~55% in pockmark sediments). Other frequent groups (e.g., AR15, AR20) are likewise symbiotic or parasitic; the latter, linked to groundwater (Castelle et al., 2015), underscores the influence of SGD in the Gulf of Gdańsk.

### 4.4 Influence of SGD and pockmark activity on marine pore waters and GDGT production

The elevated methanogen populations observed in our dataset (supplementary material Fig. S8) may be influenced by freshwater inputs associated with SGD, as methanogenic archaea can be more abundant under lower-salinity conditions along estuarine gradients, as demonstrated by Li et al. (2022). However, the effects of SGD are highly site-specific; the MET1 area and the MET4 pockmark are subject to differing degrees of freshwater infiltration (supplementary material Table S1). In the Gdańsk Basin, freshwater inflow further dilutes the already low chloride and sulphate concentrations (Idczak et al., 2020; Brodecka-Goluch et al., 2022; Łukawska-Matuszewska and Dwornik, 2025). Idczak et al. (2020) and Brodecka-Goluch et al. (2022) reported fluctuating low-oxygen to anoxic conditions in the bottom waters (MET1 area, MET3), promoting steep redox gradients which, together with sulphate depletion, favour methanogenesis. This may account for the high GDGT-0 concentrations (supplementary material Fig. S3). In addition, high terrestrial (MET1) or marine organic matter input (MET3, MET4) (estimated TOC levels; Fig. 2), enhanced by anthropogenic contamination, creates favourable conditions for intensive organic matter mineralisation and methanogenesis.

Following the SGD-focused framework of Purkamo et al. (2022), SGD-driven advection can compress redox and reaction zones into the uppermost centimetres, reduce organic matter accumulation, and suppress SMTZ development. In such active pockmarks, archaeal

https://doi.org/10.5194/egusphere-2026-519
Preprint. Discussion started: 4 February 2026


communities are dominated by AOA (Purkamo et al., 2022). Conversely, inactive pockmarks dominated by diffusion accumulate organic-rich fine-grained sediments and are characterised by sulphate reduction and methanogenesis, with methanogens prominent in the archaeal community. This suggests that advection, typical of active pockmarks, dominates in the MET1 area, whereas diffusion governs the inactive MET3, and that MET4 is probably not sufficiently active, as its iGDGT and archaeal abundance trends resemble those of MET3.

Microbial activity hotspots typically develop at interfaces and mixing zones (Stegen et al., 2016). The elevated archaeal abundances (particularly methanogenic and methanotrophic groups; Fig. 6; supplementary material Fig. S7, S8) and elevated iGDGT concentrations (Fig. 2, 4) observed at MET4 and in the MET1 area likely result from SGD–marine water mixing within a shallow redox-transition layer, where freshened groundwater mixes with marine porewater. This mixing occurs immediately below the sediment–water interface (SWI) or within a few decimetres of the seafloor (depending on hydrostatic conditions), sharpening redox gradients (within ~40 cm; Idczak et al., 2020; Brodecka-Goluch et al., 2022), which corresponds well with the elevated iGDGT concentrations detected in the upper 45 cm. Additionally, Jaśniewicz et al. (2019) noted the mechanical displacement of sub-bottom stratification and the disruption of sediment layering caused by gas bubbles in the sediments of the Gdańsk Basin. Furthermore, bottom currents likely redistribute pockmark-discharged sediments, particularly in the MET1 area, where typical pockmark deposits are absent (Idczak et al., 2020). The elevated crenarchaeol concentrations in the upper 45 cm, therefore likely reflect a combination of deposition/export and near-surface retention, as well as sustained local production under fluctuating salinity–redox conditions in the advective flushing sediment layer, together with redistribution along fluid-ventilation pathways.

Average OH-GDGT% values are broadly consistent with those reported for Baltic Sea surface sediments by Sinninghe Damsté et al. (2022). Non-pockmark sediments and MET3/MET4 cluster around the central Baltic range reported by Sinninghe Damsté et al. (2022) and the Skagerrak Sea (Kaiser and Arz, 2016), whereas MET1 pockmark samples approach the higher OH-GDGT% values previously reported for the Gulf of Finland or the Bothnian Sea. Differences are more pronounced between the MET1 area and MET3/MET4 than between pockmark and non-pockmark sediments. As OH-GDGT% distributions can be affected by salinity changes and lateral sediment influx (Sinninghe Damsté et al., 2022), we interpret these inter-site contrasts as reflecting SGD-shaped hydrography and ecology rather than a simple methane versus non-methane differentiation.

RI-OH and RI-OH′ fall within the Baltic/Skagerrak surface-sediment ranges (Sinninghe Damsté et al., 2022). Slightly higher RI-OH′ values in non-pockmark sediments likely reflect shifts along the brackish–freshwater–marine continuum and/or sediment sourcing effects. Salinity is a primary control on OH-GDGT behaviour in the Baltic Sea (Sinninghe Damsté et al., 2022), but recent work shows that OH-GDGT distributions also respond strongly to other non-thermal variables, including nitrate availability and water-column stratification (Harning and Sepúlveda, 2024), meaning that RI-OH/RI-OH′ shifts can reflect ecological factors. The most defensible biological interpretation is that OH-GDGTs largely track AOA, namely Nitrososphaeria, as they are observed in culture studies of Nitrosopumilales (Sinninghe Damsté et al., 2022). In the analysed dataset, OH-GDGTs covary tightly with crenarchaeol, as in previous research by Kaiser and Arz (2016).

## 5 Conclusions

https://doi.org/10.5194/egusphere-2026-519
Preprint. Discussion started: 4 February 2026


This study presents the first integrated analysis of archaeal 16S rRNA community profiles, sedimentary iGDGT/OH-GDGT distributions, and correlation network for methane pockmarks in the Gdańsk Basin. Pockmarks host a more diverse and abundant archaeal community than non-pockmark reference sites, functioning as tightly coupled metabolic systems in which multiple archaeal groups operate synergistically, whereas reference sites exhibit more independent, niche-partitioned ecological structures. Although *Methanosarcina* predominates across all horizons due to its metabolic versatility, vertical shifts in methanogenic taxa reflect community responses to changes in organic matter quality and sediment depth.

Despite the methane-rich environment, evidence for anaerobic oxidation of methane (AOM) remains limited. Low Methane Index values and near-absence of ANME-1 confirm previously reported thin, shallow sulphate–methane transition zone, though ANME-2b and ANME-3 are the most abundant methanotrophs in pockmarks. AOM may also rely on alternative electron acceptors (e.g., *Ca. Methanoperedens*). Low GDGT-0/cren and GDGT-2/cren ratios indicate that ammonia-oxidising archaea, particularly *Nitrosopumilus*, dominate the GDGT pool and obscure the methanogenic signal, highlighting the limited reliability of GDGT-based proxies for diagnosing AOM in environments with low ANME-1 abundance.

Results suggest that submarine groundwater discharge and pockmark activity drive geochemical conditions and microbial distribution. Mixing of freshened groundwater with marine porewater, potentially combined with gas ebullition, generates microbial activity hotspots (marked by iGDGT concentration maxima) and disrupts sub-bottom stratification. Contrasts between active advective systems (MET1) and inactive or diffusive systems (MET3, MET4) influence organic matter accumulation and archaeal community structure, and these effects could be further investigated through porewater analyses of chloride and methane profiles.

OH-GDGT distribution primarily reflects AOA populations and, to a lesser extent, site-specific hydrographic conditions associated with SGD — including salinity variations and lateral sediment influx — rather than methane seepage. In complex estuarine settings like the Gdańsk Basin, freshwater infiltration, fluid-transport mechanisms, redox fluctuations, and organic matter input exert stronger short-term control on archaeal tetraether lipid signatures than methane alone.

To establish AOM occurrence and identify responsible ANME clades, future investigations should incorporate methane-cycling tracers independent of GDGT-ratio frameworks, including hydrocarbon and ether-lipid biomarkers associated with ANME lineages (e.g., crocetane, PMI, archaeol, hydroxyarchaeol), ideally with compound-specific stable carbon isotope measurements to detect $^{13}C$-depleted methane-derived signatures. Targeted functional gene and transcriptomic analyses (e.g., *mcrA* abundance and expression) would provide activity-based constraints on methanotrophy. These approaches would differentiate between (i) ANME-2/ANME-3-dominated communities actively mediating AOM yet contributing minimally to bulk iGDGT concentrations, and (ii) limited AOM activity where GDGT distributions are governed by biomarker synthesis of Nitrososphaeria and other methane-cycling archaea. Additionally, both core lipids and intact polar lipids of GDGTs should be measured in the water column to understand GDGT production, transport, and preservation in sediment, as only core lipids were measured here, which accumulate over longer timescales. To understand bacteria's contribution to these gas systems, brGDGTs and 16S rRNA community profiles should be investigated.

https://doi.org/10.5194/egusphere-2026-519
Preprint. Discussion started: 4 February 2026


This study underscores the need for multi-proxy and multi-omic approaches to disentangle active lipid production from preserved diagenetic signals. Combining GDGTs with other biomarkers (e.g., crocetane, archaeol), isotopic analyses, and metagenomic and transcriptomic data will enable more accurate reconstruction of methane cycling and redox dynamics. Such approaches will improve the application of lipid proxies in the Baltic Sea and provide broader insights into seep ecosystems worldwide, where SGD, methane seepage, and dynamic geochemistry shape microbial ecology and biogeochemical fluxes.

*Data availability.* All iGDGT data is available in the repository 10.5281/zenodo.18414700.

*Author contributions.* IDMS and MS designed the research; IDMS evaluated the geochemical and microbiological data; AB, ABG, and KLM collected the samples; AB prepared the microbiological dataset; IDMS and AB performed the statistical analyses; IDMS wrote the manuscript; FP and MS reviewed and edited the manuscript.

*Competing interests.* The contact author has declared that none of the authors has any competing interests.

*Acknowledgements.* This study was partially funded by the Elsevier Research Scholarship (awarded to IDMS). IDMS is grateful to the Organic Geochemistry Group (Utrecht University) for assistance with analyses. AB, ABG, and KLM thank the captain and crew of RV *Oceanograf* for their help during the cruises. Paweł Działak is thanked for isolating material for DNA analysis.

## References

Aitchison, J.: The statistical analysis of compositional data, Journal of the Royal Statistical Society: Series B (Methodological), 44, 139–160, https://doi.org/10.1111/j.2517-6161.1982.tb01195.x, 1982.

Bale, N. J., Palatinszky, M., Rijpstra, W. I. C., Herbold, C. W., Wagner, M., and Sinninghe Damsté, J. S.: Membrane lipid composition of the moderately thermophilic ammonia-oxidizing archaeon "Candidatus Nitrosotenuis uzonensis" at different growth temperatures, Applied and Environmental Microbiology, 85, e01332-19, https://doi.org/10.1128/AEM.01332-19, 2019.

Bauersachs, T., Weidenbach, K., Schmitz, R. A., and Schwark, L.: Distribution of glycerol ether lipids in halophilic, methanogenic and hyperthermophilic archaea, Organic Geochemistry, 83–84, 101–108, https://doi.org/10.1016/j.orggeochem.2015.03.009, 2015.

Baxter, A. J., van Bree, L. G. J., Peterse, F., Hopmans, E. C., Villanueva, L., Verschuren, D., and Sinninghe Damsté, J. S.: Seasonal and multi-annual variation in the abundance of isoprenoid GDGT membrane lipids and their producers in the water column of a meromictic equatorial crater lake (Lake Chala, East Africa), Quaternary Science Reviews, 273, 107263, https://doi.org/10.1016/j.quascirev.2021.107263, 2021.

Baxter, B. K. and Zalar, P.: The extremophiles of Great Salt Lake: Complex microbiology in a dynamic hypersaline ecosystem, in: Model Ecosystems in Extreme Environments, edited by: Seckbach, J. and Rampelotto, P., Academic Press, 57–99, https://doi.org/10.1016/B978-0-12-812742-1.00004-0, 2019.

https://doi.org/10.5194/egusphere-2026-519
Preprint. Discussion started: 4 February 2026


950 Berg, C., Listmann, L., Vandieken, V., Vogts, A., and Jürgens, K.: Chemoautotrophic growth
951 of ammonia-oxidizing Thaumarchaeota enriched from a pelagic redox gradient in the Baltic
952 Sea, Frontiers in Microbiology, 5, https://doi.org/10.3389/fmicb.2014.00786, 2015a.

953 Berg, C., Vandieken, V., Thamdrup, B., and Jürgens, K.: Significance of archaeal nitrification
954 in hypoxic waters of the Baltic Sea, The ISME Journal, 9, 1319–1332,
955 https://doi.org/10.1038/ismej.2014.218, 2015b.

956 Besseling, M. A., Hopmans, E. C., Boschman, R. C., Sinninghe Damsté, J. S., and
957 Villanueva, L.: Benthic archaea as potential sources of tetraether membrane lipids in
958 sediments across an oxygen minimum zone, Biogeosciences, 15, 4047–4064,
959 https://doi.org/10.5194/bg-15-4047-2018, 2018.

960 Besseling, M. A., Hopmans, E. C., Bale, N. J., Schouten, S., Damsté, J. S. S., and Villanueva,
961 L.: The absence of intact polar lipid-derived GDGTs in marine waters dominated by Marine
962 Group II: Implications for lipid biosynthesis in Archaea, Scientific Reports, 10, 294,
963 https://doi.org/10.1038/s41598-019-57035-0, 2020.

964 Bijl, P. K., Śliwińska, K. K., Duncan, B., Huguet, A., Naeher, S., Rattanasriampaipong, R.,
965 Sosa-Montes de Oca, C., Auderset, A., Berke, M. A., Kim, B. S., Davtian, N., Dunkley Jones,
966 T., Eefting, D. D., Elling, F. J., Fenies, P., Inglis, G. N., O'Connor, L., Pancost, R. D.,
967 Peterse, F., Rice, A., Sluijs, A., Varma, D., Xiao, W., and Zhang, Y. G.: Reviews and
968 syntheses: Best practices for the application of marine GDGTs as proxy for
969 paleotemperatures: sampling, processing, analyses, interpretation, and archiving protocols,
970 Biogeosciences, 22, 6465–6508, https://doi.org/10.5194/bg-22-6465-2025, 2025.

971 Blaga, C. I., Reichart, G.-J., Heiri, O., and Sinninghe Damsté, J. S.: Tetraether membrane
972 lipid distributions in water-column particulate matter and sediments: a study of 47 European
973 lakes along a north–south transect, Journal of Paleolimnology, 41, 523–540,
974 https://doi.org/10.1007/s10933-008-9242-2, 2009.

975 Blainey, P. C., Mosier, A. C., Potanina, A., Francis, C. A., and Quake, S. R.: Genome of a
976 low-salinity ammonia-oxidizing archaeon determined by single-cell and metagenomic
977 analysis, PLoS One, 6, e16626, https://doi.org/10.1371/journal.pone.0016626, 2011.

978 Blewett, J., Elling, F. J., Naafs, B. D. A., Kattein, L., Evans, T. W., Lauretano, V., Gallego-
979 Sala, A. V., Pancost, R. D., and Pearson, A.: Metabolic and ecological controls on the stable
980 carbon isotopic composition of archaeal (isoGDGT and BDGT) and bacterial (brGDGT)
981 lipids in wetlands and lignites, Geochimica et Cosmochimica Acta, 320, 1–25,
982 https://doi.org/10.1016/j.gca.2021.12.023, 2022.

983 Blondel, V. D., Guillaume, J.-L., Lambiotte, R., and Lefebvre, E.: Fast unfolding of
984 communities in large networks, Journal of Statistical Mechanics: Theory and Experiment,
985 2008, P10008, https://doi.org/10.1088/1742-5468/2008/10/P10008, 2008.

986 Boetius, A., Ravenschlag, K., Schubert, C. J., Rickert, D., Widdel, F., Gieseke, A., Amann,
987 R., Jørgensen, B. B., Witte, U., and Pfannkuche, O.: A marine microbial consortium
988 apparently mediating anaerobic oxidation of methane, Nature, 407, 623–626,
989 https://doi.org/10.1038/35036572, 2000.

990 van den Boogaart, K. G., Tolosana-Delgado, R., and Bren, M.: Package "compositions":
991 Compositional Data Analysis, 2024.

https://doi.org/10.5194/egusphere-2026-519
Preprint. Discussion started: 4 February 2026


Brick, S., Niggemann, J., Reckhardt, A., Könneke, M., and Engelen, B.: Interstitial microbial communities of coastal sediments are dominated by Nanoarchaeota, Frontiers in Microbiology, 16, 1532193, https://doi.org/10.3389/fmicb.2025.1532193, 2025.

Brocławik, O., Łukawska-Matuszewska, K., Brodecka-Goluch, A., and Bolałek, J.: Impact of methane occurrence on iron speciation in the sediments of the Gdansk Basin (Southern Baltic Sea), Science of The Total Environment, 721, 137718, https://doi.org/10.1016/j.scitotenv.2020.137718, 2020.

Brodecka, A., Majewski, P., Bolałek, J., and Klusek, Z.: Geochemical and acoustic evidence for the occurrence of methane in sediments of the Polish sector of the southern Baltic Sea*, Oceanologia, 55, 951–978, https://doi.org/10.5697/oc.55-4.951, 2013.

Brodecka-Goluch, A., Łukawska-Matuszewska, K., Kotarba, M. J., Borkowski, A., Idczak, J., and Bolałek, J.: Biogeochemistry of three different shallow gas systems in continental shelf sediments of the South-Eastern Baltic Sea (Gulf of Gdańsk): Carbon cycling, origin of methane and microbial community composition, Chemical Geology, 597, 120799, https://doi.org/10.1016/j.chemgeo.2022.120799, 2022.

Burnett, W. C., Bokuniewicz, H., Huettel, M., Moore, W. S., and Taniguchi, M.: Groundwater and pore water inputs to the coastal zone, Biogeochemistry, 66, 3–33, https://doi.org/10.1023/B:BIOG.0000006066.21240.53, 2003.

Burnett, W. C., Aggarwal, P. K., Aureli, A., Bokuniewicz, H., Cable, J. E., Charette, M. A., Kontar, E., Krupa, S., Kulkarni, K. M., Loveless, A., Moore, W. S., Oberdorfer, J. A., Oliveira, J., Ozyurt, N., Povinec, P., Privitera, A. M. G., Rajar, R., Ramessur, R. T., Scholten, J., Stieglitz, T., Taniguchi, M., and Turner, J. V.: Quantifying submarine groundwater discharge in the coastal zone via multiple methods, Science of The Total Environment, 367, 498–543, https://doi.org/10.1016/j.scitotenv.2006.05.009, 2006.

Bussmann, I. and Suess, E.: Groundwater seepage in Eckernförde Bay (Western Baltic Sea): Effect on methane and salinity distribution of the water column, Continental Shelf Research, 18, 1795–1806, https://doi.org/10.1016/S0278-4343(98)00058-2, 1998.

Callow, B., Bull, J. M., Provenzano, G., Böttner, C., Birinci, H., Robinson, A. H., Henstock, T. J., Minshull, T. A., Bayrakci, G., Lichtschlag, A., Roche, B., Yilo, N., Gehrmann, R., Karstens, J., Falcon-Suarez, I. H., and Berndt, C.: Seismic chimney characterisation in the North Sea – Implications for pockmark formation and shallow gas migration, Marine and Petroleum Geology, 133, 105301, https://doi.org/10.1016/j.marpetgeo.2021.105301, 2021.

Carrier, V., Svenning, M. M., Gründger, F., Niemann, H., Dessandier, P.-A., Panieri, G., and Kalenitchenko, D.: The impact of methane on microbial communities at marine Arctic gas hydrate bearing sediment, Frontiers in Microbiology, 11, https://doi.org/10.3389/fmicb.2020.01932, 2020.

Castelle, C. J., Wrighton, K. C., Thomas, B. C., Hug, L. A., Brown, C. T., Wilkins, M. J., Frischkorn, K. R., Tringe, S. G., Singh, A., Markillie, L. M., Taylor, R. C., Williams, K. H., and Banfield, J. F.: Genomic expansion of domain Archaea highlights roles for organisms from new phyla in anaerobic carbon cycling, Current Biology, 25, 690–701, https://doi.org/10.1016/j.cub.2015.01.014, 2015.

https://doi.org/10.5194/egusphere-2026-519
Preprint. Discussion started: 4 February 2026


Chen, S., Zhou, Y., Chen, Y., and Gu, J.: fastp: an ultra-fast all-in-one FASTQ preprocessor, Bioinformatics, 34, i884–i890, https://doi.org/10.1093/bioinformatics/bty560, 2018.

Conklin, A., Stensel, H. D., and Ferguson, J.: Growth kinetics and competition between Methanosarcina and Methanosaeta in mesophilic anaerobic digestion, Water Environment Research, 78, 486–496, https://doi.org/10.2175/106143006X95393, 2006.

De Rosa, M., De Rosa, S., Gambacorta, A., Minale, L., and Bu'lock, J. D.: Chemical structure of the ether lipids of thermophilic acidophilic bacteria of the Caldariella group, Phytochemistry, 16, 1961–1965, https://doi.org/10.1016/0031-9422(77)80105-2, 1977.

Díaz-Mendoza, G. A., Krämer, K., von Rönn, G. A., Schwarzer, K., Heinrich, C., Reimers, H.-C., and Winter, C.: Circular structures on the seabed: differentiating between natural and anthropogenic origins—Examples from the Southwestern Baltic Sea, Frontiers in Earth Science, 11, 1170787, 2023.

Ehlert von Ahn, C. M., Dellwig, O., Szymczycha, B., Kotwicki, L., Rooze, J., Endler, R., Escher, P., Schmiedinger, I., Sültenfuß, J., Diak, M., Gehre, M., Struck, U., Vogler, S., and Böttcher, M. E.: Submarine groundwater discharge into a semi-enclosed coastal bay of the southern Baltic Sea: A multi-method approach, Oceanologia, 66, 111–138, https://doi.org/10.1016/j.oceano.2024.01.001, 2024.

Elling, F. J., Könneke, M., Nicol, G. W., Stieglmeier, M., Bayer, B., Spieck, E., de la Torre, J. R., Becker, K. W., Thomm, M., Prosser, J. I., Herndl, G. J., Schleper, C., and Hinrichs, K.-U.: Chemotaxonomic characterisation of the thaumarchaeal lipidome, Environmental Microbiology, 19, 2681–2700, https://doi.org/10.1111/1462-2920.13759, 2017.

Ettwig, K. F., Zhu, B., Speth, D., Keltjens, J. T., Jetten, M. S. M., and Kartal, B.: Archaea catalyze iron-dependent anaerobic oxidation of methane, Proceedings of the National Academy of Sciences, 113, 12792–12796, https://doi.org/10.1073/pnas.1609534113, 2016.

Eurostat/GISCO, "Countries (Administrative units) — polygons (RG)" [dataset], scale 1:1M, 2024, EPSG:4326 (file: CNTR_RG_01M_2024_4326), European Commission (Eurostat) / GISCO. https://ec.europa.eu/eurostat/web/gisco/geodata/administrative-units (Accessed January 30, 2026).

Galagan, J. E., Nusbaum, C., Roy, A., Endrizzi, M. G., Macdonald, P., FitzHugh, W., Calvo, S., Engels, R., Smirnov, S., Atnoor, D., Brown, A., Allen, N., Naylor, J., Stange-Thomann, N., DeArellano, K., Johnson, R., Linton, L., McEwan, P., McKernan, K., Talamas, J., Tirrell, A., Ye, W., Zimmer, A., Barber, R. D., Cann, I., Graham, D. E., Grahame, D. A., Guss, A. M., Hedderich, R., Ingram-Smith, C., Kuettner, H. C., Krzycki, J. A., Leigh, J. A., Li, W., Liu, J., Mukhopadhyay, B., Reeve, J. N., Smith, K., Springer, T. A., Umayam, L. A., White, O., White, R. H., Conway de Macario, E., Ferry, J. G., Jarrell, K. F., Jing, H., Macario, A. J. L., Paulsen, I., Pritchett, M., Sowers, K. R., Swanson, R. V., Zinder, S. H., Lander, E., Metcalf, W. W., and Birren, B.: The genome of M. acetivorans reveals extensive metabolic and physiological diversity, Genome Research, 12, 532–542, https://doi.org/10.1101/gr.223902, 2002.

Gloor, G. B., Macklaim, J. M., Pawlowsky-Glahn, V., and Egozcue, J. J.: Microbiome datasets are compositional: and this is not optional, Frontiers in Microbiology, 8, 2224, 2017.

https://doi.org/10.5194/egusphere-2026-519
Preprint. Discussion started: 4 February 2026


Guan, H., Liu, L., Birgel, D., Peckmann, J., Feng, D., and Li, S.: Hydroxylated GDGTs-0 in marine methane seep environments: A putative indicator for archaeal methanogenesis, Organic Geochemistry, 198, 104862, https://doi.org/10.1016/j.orggeochem.2024.104862, 2024.

Harning, D. J. and Sepúlveda, J.: Impact of non-thermal variables on hydroxylated GDGT distributions around Iceland, Front. Earth Sci., 12, https://doi.org/10.3389/feart.2024.1430441, 2024.

Haroon, M. F., Hu, S., Shi, Y., Imelfort, M., Keller, J., Hugenholtz, P., Yuan, Z., and Tyson, G. W.: Anaerobic oxidation of methane coupled to nitrate reduction in a novel archaeal lineage, Nature, 500, 567–570, https://doi.org/10.1038/nature12375, 2013.

HELCOM Secretariat, "Baltic Sea Bathymetry Database (BSBD)" [dataset], 500 m resolution bathymetric model (GeoTIFF; v0.91), HELCOM Metadata Catalogue, metadata record ID: 8b46e4c7-f911-44ab-89e6-2c8b8d9fa2c0. https://metadata.helcom.fi/geonetwork/srv/eng/catalog.search#/metadata/8b46e4c7-f911-44ab-89e6-2c8b8d9fa2c0 (Accessed January 30, 2026).

Hoffmann, J. J. L., Schneider von Deimling, J., Schröder, J. F., Schmidt, M., Held, P., Crutchley, G. J., Scholten, J., and Gorman, A. R.: Complex eyed pockmarks and submarine groundwater discharge revealed by acoustic data and sediment cores in Eckernförde Bay, SW Baltic Sea, Geochemistry, Geophysics, Geosystems, 21, e2019GC008825, https://doi.org/10.1029/2019GC008825, 2020.

Hovland, M. and Judd, A. G.: Seabed Pockmarks and Seepages. Impact on Geology, Biology and the Marine Environment, Graham & Trotman (Kluwer), London, Dordrecht, Boston, 293 pp., 1988.

Hovland, M., Gardner, J. V., and Judd, A. G.: The significance of pockmarks to understanding fluid flow processes and geohazards, Geofluids, 2, 127–136, 2002.

Huguet, C., Hopmans, E. C., Febo-Ayala, W., Thompson, D. H., Sinninghe Damsté, J. S., and Schouten, S.: An improved method to determine the absolute abundance of glycerol dibiphytanyl glycerol tetraether lipids, Organic Geochemistry, 37, 1036–1041, https://doi.org/10.1016/j.orggeochem.2006.05.008, 2006.

Huguet, C., Fietz, S., and Rosell-Melé, A.: Global distribution patterns of hydroxy glycerol dialkyl glycerol tetraethers, Organic Geochemistry, 57, 107–118, https://doi.org/10.1016/j.orggeochem.2013.01.010, 2013.

Idczak, J., Brodecka-Goluch, A., Łukawska-Matuszewska, K., Graca, B., Gorska, N., Klusek, Z., Pezacki, P. D., and Bolałek, J.: A geophysical, geochemical and microbiological study of a newly discovered pockmark with active gas seepage and submarine groundwater discharge (MET1-BH, central Gulf of Gdańsk, southern Baltic Sea), Science of The Total Environment, 742, 140306, https://doi.org/10.1016/j.scitotenv.2020.140306, 2020.

Inglis, G. N., Farnsworth, A., Lunt, D., Foster, G. L., Hollis, C. J., Pagani, M., Jardine, P. E., Pearson, P. N., Markwick, P., Galsworthy, A. M. J., Raynham, L., Taylor, Kyle. W. R., and Pancost, R. D.: Descent toward the Icehouse: Eocene sea surface cooling inferred from

https://doi.org/10.5194/egusphere-2026-519
Preprint. Discussion started: 4 February 2026


GDGT distributions, Paleoceanography, 30, 1000–1020, https://doi.org/10.1002/2014PA002723, 2015.

Jakobs, G., Labrenz, M., Rehder, G., Hietanen, S., Kießlich, K., Vogts, A., Blumenberg, M., and Schmale, O.: A boreactor approach to investigate the linkage between methane oxidation and nitrate/nitrite reduction in the pelagic oxic-anoxic transition zone of the Central Baltic Sea, Frontiers in Marine Science, 3, https://doi.org/10.3389/fmars.2016.00145, 2016.

Jakobsson, M., O'Regan, M., Mörth, C.-M., Stranne, C., Weidner, E., Hansson, J., Gyllencreutz, R., Humborg, C., Elfwing, T., Norkko, A., Norkko, J., Nilsson, B., and Sjöström, A.: Potential links between Baltic Sea submarine terraces and groundwater seeping, Earth Surface Dynamics, 8, 1–15, https://doi.org/10.5194/esurf-8-1-2020, 2020.

Jäntti, H., Ward, B. B., Dippner, J. W., and Hietanen, S.: Nitrification and the ammonia-oxidizing communities in the central Baltic Sea water column, Estuarine, Coastal and Shelf Science, 202, 280–289, https://doi.org/10.1016/j.ecss.2018.01.019, 2018.

Jaśniewicz, D., Klusek, Z., Brodecka-Goluch, A., and Bolałek, J.: Acoustic investigations of shallow gas in the southern Baltic Sea (Polish Exclusive Economic Zone): a review, Geo-Marine Letters, 39, 1–17, https://doi.org/10.1007/s00367-018-0555-5, 2019.

Jaworowski, K., Wagner, R., Modliski, Z., Pokorski, J., Sokołowski, J., and Sokołowski, A.: Marine ecogeology in semi-closed basin: case study on a threat of geogenic pollution of the southern Baltic Sea (Polish Exclusive Economic Zone), Geological Quarterly, 54, 267–288, 2010.

Jensen, J. B., Kuijpers, A., Bennike, O., Laier, T., and Werner, F.: New geological aspects for freshwater seepage and formation in Eckernförde Bay, western Baltic, Continental Shelf Research, 22, 2159–2173, https://doi.org/10.1016/S0278-4343(02)00076-6, 2002.

Kaiser, J. and Arz, H. W.: Sources of sedimentary biomarkers and proxies with potential paleoenvironmental significance for the Baltic Sea, Continental Shelf Research, 122, 102–119, https://doi.org/10.1016/j.csr.2016.03.020, 2016.

Kim, B. and Zhang, Y. G.: Methane Index: Towards a quantitative archaeal lipid biomarker proxy for reconstructing marine sedimentary methane fluxes, Geochimica et Cosmochimica Acta, 354, 74–87, https://doi.org/10.1016/j.gca.2023.06.008, 2023.

King, L. H. and MacLean, B.: Pockmarks on the Scotian Shelf, GSA Bulletin, 81, 3141–3148, 1970.

Knittel, K. and Boetius, A.: Anaerobic oxidation of methane: progress with an unknown process, Annual Review of Microbiology, 63, 311–334, https://doi.org/10.1146/annurev.micro.61.080706.093130, 2009.

Koga, Y., Nishihara, M., Morii, H., and Akagawa-Matsushita, M.: Ether polar lipids of methanogenic bacteria: structures, comparative aspects, and biosyntheses, Microbiological Reviews, 57, 164–182, https://doi.org/10.1128/mr.57.1.164-182.1993, 1993.

Kotarba, M. J.: Origin of hydrocarbon gases accumulated in the Middle Cambrian reservoirs of the Polish part of the Baltic region, Geological Quarterly, 54, 197–204, 2010.

https://doi.org/10.5194/egusphere-2026-519
Preprint. Discussion started: 4 February 2026


Kotarba, M. J. and Lewan, M. D.: Sources of natural gases in Middle Cambrian reservoirs in Polish and Lithuanian Baltic Basin as determined by stable isotopes and hydrous pyrolysis of Lower Palaeozoic source rocks, Chemical Geology, 345, 62–76, https://doi.org/10.1016/j.chemgeo.2013.02.023, 2013.

Kotarba, M. J. and Nagao, K.: Molecular and isotopic compositions and origin of natural gases from Cambrian and Carboniferous-Lower Permian reservoirs of the onshore Polish Baltic region, International Journal of Earth Sciences, 104, 241–261, https://doi.org/10.1007/s00531-014-1063-0, 2015.

Kreuzburg, M., Scholten, J., Hsu, F.-H., Liebetrau, V., Sültenfuß, J., Rapaglia, J., and Schlüter, M.: Submarine groundwater discharge-derived nutrient fluxes in Eckernförde Bay (Western Baltic Sea), Estuaries and Coasts, 46, 1190–1207, https://doi.org/10.1007/s12237-023-01202-0, 2023.

Kuliński, K., Rehder, G., Asmala, E., Bartosova, A., Carstensen, J., Gustafsson, B., Hall, P. O. J., Humborg, C., Jilbert, T., Jürgens, K., Meier, H. E. M., Müller-Karulis, B., Naumann, M., Olesen, J. E., Savchuk, O., Schramm, A., Slomp, C. P., Sofiev, M., Sobek, A., Szymczycha, B., and Undeman, E.: Biogeochemical functioning of the Baltic Sea, Earth System Dynamics, 13, 633–685, https://doi.org/10.5194/esd-13-633-2022, 2022.

Kurowski, S., Łukawska-Matuszewska, K., Čović, A., Jozić, D., and Brodecka-Goluch, A.: Effects of pockmark activity on iron cycling and mineral composition in continental shelf sediments (southern Baltic Sea), Biogeochemistry, 167, 135–154, https://doi.org/10.1007/s10533-024-01127-1, 2024.

Labrenz, M., Sintes, E., Toetzke, F., Zumsteg, A., Herndl, G. J., Seidler, M., and Jürgens, K.: Relevance of a crenarchaeotal subcluster related to Candidatus Nitrosopumilus maritimus to ammonia oxidation in the suboxic zone of the central Baltic Sea, The ISME Journal, 4, 1496–1508, https://doi.org/10.1038/ismej.2010.78, 2010.

Lee, D.-H., Kim, J.-H., Lee, Y. M., Stadnitskaia, A., Jin, Y. K., Niemann, H., Kim, Y.-G., and Shin, K.-H.: Biogeochemical evidence of anaerobic methane oxidation on active submarine mud volcanoes on the continental slope of the Canadian Beaufort Sea, Biogeosciences, 15, 7419–7433, https://doi.org/10.5194/bg-15-7419-2018, 2018.

Lengger, S. K., Kraaij, M., Tjallingii, R., Baas, M., Stuut, J.-B., Hopmans, E. C., Sinninghe Damsté, J. S., and Schouten, S.: Differential degradation of intact polar and core glycerol dialkyl glycerol tetraether lipids upon post-depositional oxidation, Organic Geochemistry, 65, 83–93, https://doi.org/10.1016/j.orggeochem.2013.10.004, 2013.

Leu, A. O., Cai, C., McIlroy, S. J., Southam, G., Orphan, V. J., Yuan, Z., Hu, S., and Tyson, G. W.: Anaerobic methane oxidation coupled to manganese reduction by members of the Methanoperedenaceae, The ISME Journal, 14, 1030–1041, https://doi.org/10.1038/s41396-020-0590-x, 2020.

Li, X., Li, Y., Gao, D., Liu, M., and Hou, L.: Methane production linked to organic matter molecule and methanogenic community in estuarine benthic sediments, Journal of Geophysical Research: Biogeosciences, 127, e2022JG007236, https://doi.org/10.1029/2022JG007236, 2022.

https://doi.org/10.5194/egusphere-2026-519
Preprint. Discussion started: 4 February 2026


Liu, Q., Charette, M. A., Breier, C. F., Henderson, P. B., McCorkle, D. C., Martin, W., and Dai, M.: Carbonate system biogeochemistry in a subterranean estuary – Waquoit Bay, USA, Geochimica et Cosmochimica Acta, 203, 422–439, https://doi.org/10.1016/j.gca.2017.01.041, 2017.

Liu, X.-L., Summons, R. E., and Hinrichs, K.-U.: Extending the known range of glycerol ether lipids in the environment: structural assignments based on tandem mass spectral fragmentation patterns, Rapid Communications in Mass Spectrometry, 26, 2295–2302, https://doi.org/10.1002/rcm.6355, 2012.

Lu, J., Breitwieser, F. P., Thielen, P., and Salzberg, S. L.: Bracken: estimating species abundance in metagenomics data, PeerJ Computer Science, 3, e104, https://doi.org/10.7717/peerj-cs.104, 2017.

Lu, J., Rincon, N., Wood, D. E., Breitwieser, F. P., Pockrandt, C., Langmead, B., Salzberg, S. L., and Steinegger, M.: Metagenome analysis using the Kraken software suite, Nature Protocols, 17, 2815–2839, https://doi.org/10.1038/s41596-022-00738-y, 2022.

Lü, X., Liu, X.-L., Elling, F. J., Yang, H., Xie, S., Song, J., Li, X., Yuan, H., Li, N., and Hinrichs, K.-U.: Hydroxylated isoprenoid GDGTs in Chinese coastal seas and their potential as a paleotemperature proxy for mid-to-low latitude marginal seas, Organic Geochemistry, 89–90, 31–43, https://doi.org/10.1016/j.orggeochem.2015.10.004, 2015.

Łukawska-Matuszewska, K. and Dwornik, M.: Early diagenesis in anoxic sediments of the Gulf of Gdańsk (southern Baltic Sea): Implications for porewater chemistry and benthic flux of carbonate alkalinity, Frontiers in Earth Science, 13, https://doi.org/10.3389/feart.2025.1593031, 2025.

Łukawska-Matuszewska, K., Kiełczewska, J., and Bolałek, J.: Factors controlling spatial distributions and relationships of carbon, nitrogen, phosphorus and sulphur in sediments of the stratified and eutrophic Gulf of Gdansk, Continental Shelf Research, 85, 168–180, https://doi.org/10.1016/j.csr.2014.06.010, 2014.

Łukawska-Matuszewska, K., Brocławik, O., Brodecka-Goluch, A., Rzepa, G., Manecki, M., and Bolałek, J.: Biogeochemical and mineralogical effects of Fe-P-S dynamics in sediments of continental shelf sea: Impact of salinity, oxygen conditions, and catchment area characteristics, Science of The Total Environment, 807, 151035, https://doi.org/10.1016/j.scitotenv.2021.151035, 2022.

Lynes, M. M., Jay, Z. J., Kohtz, A. J., and Hatzenpichler, R.: Methylotrophic methanogenesis in the Archaeoglobi revealed by cultivation of Ca. Methanoglobus hypatiae from a Yellowstone hot spring, The ISME Journal, 18, wrae026, https://doi.org/10.1093/ismejo/wrae026, 2024.

Maeder, D. L., Anderson, I., Brettin, T. S., Bruce, D. C., Gilna, P., Han, C. S., Lapidus, A., Metcalf, W. W., Saunders, E., Tapia, R., and Sowers, K. R.: The Methanosarcina barkeri genome: comparative analysis with Methanosarcina acetivorans and Methanosarcina mazei reveals extensive rearrangement within methanosarcinal genomes, Journal of Bacteriology, 188, 7922–7931, https://doi.org/10.1128/JB.00810-06, 2006.

Majewski, P. and Klusek, Z.: Expressions of shallow gas in the Gdansk Basin, Zeszyty Naukowe Akademii Marynarki Wojennej, 52, 61–71, 2011.

https://doi.org/10.5194/egusphere-2026-519
Preprint. Discussion started: 4 February 2026


Moore, W. S.: The effect of submarine groundwater discharge on the ocean, Annual Review of Marine Science, 2, 59–88, https://doi.org/10.1146/annurev-marine-120308-081019, 2010.

Niemann, H. and Elvert, M.: Diagnostic lipid biomarker and stable carbon isotope signatures of microbial communities mediating the anaerobic oxidation of methane with sulphate, Organic Geochemistry, 39, 1668–1677, https://doi.org/10.1016/j.orggeochem.2007.11.003, 2008.

O'Reilly, S. S., Jordan, S. F., Monteys, X., Simpson, A. J., Allen, C. C. R., Szpak, M. T., Murphy, B. T., McCarron, S. G., Soong, R., Wu, B., Jenne, A., Grey, A., and Kelleher, B. P.: Production of methane and gaseous compounds by surface microbial activity in a small pockmark field, Dunmanus Bay, Ireland, Estuarine, Coastal and Shelf Science, 255, 107340, https://doi.org/10.1016/j.ecss.2021.107340, 2021.

Palarea-Albaladejo, J. and Martín-Fernández, J. A.: zCompositions — R package for multivariate imputation of left-censored data under a compositional approach, Chemometrics and Intelligent Laboratory Systems, 143, 85–96, https://doi.org/10.1016/j.chemolab.2015.02.019, 2015.

Pancost, R. D., Hopmans, E. C., and Sinninghe Damsté, J. S.: Archaeal lipids in Mediterranean cold seeps: molecular proxies for anaerobic methane oxidation, Geochimica et Cosmochimica Acta, 65, 1611–1627, https://doi.org/10.1016/S0016-7037(00)00562-7, 2001.

Petrick, B., Reuning, L., and Martínez-García, A.: Distribution of glycerol dialkyl glycerol tetraethers (GDGTs) in microbial mats from Holocene and Miocene sabkha sediments, Frontiers in Earth Science, 7, https://doi.org/10.3389/feart.2019.00310, 2019.

PGI-NRI/CBDG, "Bathymetric map of the South Baltic Sea, 1:200,000" [web map service], OGC WMS 1.3.0. Landing page: https://dane.gov.pl/en/dataset/3328/resource/51084; Service endpoint: https://cbdgmapa.pgi.gov.pl/arcgis/services/geomorze/batymetria/MapServer/WMSServer? (Accessed January 30, 2026).

Piekarek-Jankowska, H.: Hydrochemical effects of submarine groundwater discharge to the Puck Bay [Southern Baltic Sea, Poland], Geographia Polonica, 67, 103–119, 1996.

Pimenov, N. V., Ulyanova, M. O., Kanapatsky, T. A., Veslopolova, E. F., Sigalevich, P. A., and Sivkov, V. V.: Microbially mediated methane and sulfur cycling in pockmark sediments of the Gdansk Basin, Baltic Sea, Geo-Marine Letters, 30, 439–448, https://doi.org/10.1007/s00367-010-0200-4, 2010.

Pokorski, J.: Geological section through the lower Paleozoic strata of the Polish part of the Baltic region, Geological Quarterly, 54, 123–130, 2010.

Purkamo, L., von Ahn, C. M. E., Jilbert, T., Muniruzzaman, M., Bange, H. W., Jenner, A.-K., Böttcher, M. E., and Virtasalo, J. J.: Impact of submarine groundwater discharge on biogeochemistry and microbial communities in pockmarks, Geochimica et Cosmochimica Acta, 334, 14–44, https://doi.org/10.1016/j.gca.2022.06.040, 2022.

Quast, C., Pruesse, E., Yilmaz, P., Gerken, J., Schweer, T., Yarza, P., Peplies, J., and Glöckner, F. O.: The SILVA ribosomal RNA gene database project: improved data processing

https://doi.org/10.5194/egusphere-2026-519
Preprint. Discussion started: 4 February 2026


and web-based tools, Nucleic Acids Research, 41, D590–D596, https://doi.org/10.1093/nar/gks1219, 2013.

Quinn, T. P., Erb, I., Gloor, G., Notredame, C., Richardson, M. F., and Crowley, T. M.: A field guide for the compositional analysis of any-omics data, GigaScience, 8, giz107, https://doi.org/10.1093/gigascience/giz107, 2019.

R Core Team: R: A language and environment for statistical computing. R Foundation for Statistical Computing, 2023.

Reeburgh, W. S.: Oceanic methane biogeochemistry, Chemical Reviews, 107, 486–513, https://doi.org/10.1021/cr050362v, 2007.

Rinke, C., Chuvochina, M., Mussig, A. J., Chaumeil, P.-A., Davín, A. A., Waite, D. W., Whitman, W. B., Parks, D. H., and Hugenholtz, P.: A standardized archaeal taxonomy for the Genome Taxonomy Database, Nature Microbiology, 6, 946–959, https://doi.org/10.1038/s41564-021-00918-8, 2021.

Rise, L., Bellec, V. K., Chand, S., and Bøe, R.: Pockmarks in the southwestern Barents Sea and Finnmark fjords, Norwegian Journal of Geology, 94, 2014.

Rossel, P. E., Lipp, J. S., Fredricks, H. F., Arnds, J., Boetius, A., Elvert, M., and Hinrichs, K.-U.: Intact polar lipids of anaerobic methanotrophic archaea and associated bacteria, Organic Geochemistry, 39, 992–999, https://doi.org/10.1016/j.orggeochem.2008.02.021, 2008.

Ruff, S. E., Biddle, J. F., Teske, A. P., Knittel, K., Boetius, A., and Ramette, A.: Global dispersion and local diversification of the methane seep microbiome, Proceedings of the National Academy of Sciences, 112, 4015–4020, https://doi.org/10.1073/pnas.1421865112, 2015.

Schlüter, M., Sauter, E. J., Andersen, C. E., Dahlgaard, H., and Dando, P. R.: Spatial distribution and budget for submarine groundwater discharge in Eckernförde Bay (Western Baltic Sea), Limnology and Oceanography, 49, 157–167, https://doi.org/10.4319/lo.2004.49.1.0157, 2004.

Schmuck, E. A. and Paull, C. K.: Evidence for gas accumulation associated with diapirism and gas hydrates at the head of the Cape Fear Slide, Geo-Marine Letters, 13, 145–152, https://doi.org/10.1007/BF01593187, 1993.

Schouten, S., Hopmans, E. C., Pancost, R. D., and Damsté, J. S. S.: Widespread occurrence of structurally diverse tetraether membrane lipids: Evidence for the ubiquitous presence of low-temperature relatives of hyperthermophiles, Proceedings of the National Academy of Sciences, 97, 14421–14426, https://doi.org/10.1073/pnas.97.26.14421, 2000.

Schouten, S., Hopmans, E. C., Schefuß, E., and Sinninghe Damsté, J. S.: Distributional variations in marine crenarchaeotal membrane lipids: a new tool for reconstructing ancient sea water temperatures?, Earth and Planetary Science Letters, 204, 265–274, https://doi.org/10.1016/S0012-821X(02)00979-2, 2002.

Schouten, S., Hopmans, E. C., and Sinninghe Damsté, J. S.: The organic geochemistry of glycerol dialkyl glycerol tetraether lipids: A review, Organic Geochemistry, 54, 19–61, https://doi.org/10.1016/j.orggeochem.2012.09.006, 2013.

https://doi.org/10.5194/egusphere-2026-519
Preprint. Discussion started: 4 February 2026


Shaw, J., Courtney, R. C., and Currie, J. R.: Marine geology of St. George's Bay, Newfoundland, as interpreted from multibeam bathymetry and back-scatter data, Geo-Marine Letters, 17, 188–194, https://doi.org/10.1007/s003670050025, 1997.

Sinninghe Damsté, J. S., Schouten, S., Hopmans, E. C., Duin, A. C. T. van, and Geenevasen, J. A. J.: Crenarchaeol, Journal of Lipid Research, 43, 1641–1651, https://doi.org/10.1194/jlr.M200148-JLR200, 2002.

Sinninghe Damsté, J. S., Warden, L. A., Berg, C., Jürgens, K., and Moros, M.: Evaluation of the distributions of hydroxylated glycerol dibiphytanyl glycerol tetraethers (GDGTs) in Holocene Baltic Sea sediments for reconstruction of sea surface temperature: the effect of changing salinity, Climate of the Past, 18, 2271–2288, https://doi.org/10.5194/cp-18-2271-2022, 2022.

Słowakiewicz, M., Whitaker, F., Thomas, L., Tucker, M. E., Zheng, Y., Gedl, P., and Pancost, R. D.: Biogeochemistry of intertidal microbial mats from Qatar: New insights from organic matter characterisation, Organic Geochemistry, 102, 14–29, https://doi.org/10.1016/j.orggeochem.2016.09.006, 2016.

Sowers, K. R., Boone, J. E., and Gunsalus, R. P.: Disaggregation of Methanosarcina spp. and growth as single cells at elevated osmolarity, Applied and Environmental Microbiology, 59, 3832–3839, https://doi.org/10.1128/aem.59.11.3832-3839.1993, 1993.

Stadnitskaia, A., Muyzer, G., Abbas, B., Coolen, M. J. L., Hopmans, E. C., Baas, M., van Weering, T. C. E., Ivanov, M. K., Poludetkina, E., and Sinninghe Damsté, J. S.: Biomarker and 16S rDNA evidence for anaerobic oxidation of methane and related carbonate precipitation in deep-sea mud volcanoes of the Sorokin Trough, Black Sea, Marine Geology, 217, 67–96, https://doi.org/10.1016/j.margeo.2005.02.023, 2005.

Stegen, J. C., Fredrickson, J. K., Wilkins, M. J., Konopka, A. E., Nelson, W. C., Arntzen, E. V., Chrisler, W. B., Chu, R. K., Danczak, R. E., Fansler, S. J., Kennedy, D. W., Resch, C. T., and Tfaily, M.: Groundwater–surface water mixing shifts ecological assembly processes and stimulates organic carbon turnover, Nature Communications, 7, 11237, https://doi.org/10.1038/ncomms11237, 2016.

Szczepańska, T. and Uścinowicz, S.: Atlas geochemiczny południowego Bałtyku, Państwowy Instytut Geologiczny, Warszawa, 1–55 pp., 1994.

Szymczak-Żyła, M. and Lubecki, L.: Biogenic and anthropogenic sources of sedimentary organic matter in marine coastal areas: A multi-proxy approach based on bulk and molecular markers, Marine Chemistry, 239, 104069, https://doi.org/10.1016/j.marchem.2021.104069, 2022.

Szymczycha, B., Kroeger, K. D., and Pempkowiak, J.: Significance of groundwater discharge along the coast of Poland as a source of dissolved metals to the southern Baltic Sea, Marine Pollution Bulletin, 109, 151–162, https://doi.org/10.1016/j.marpolbul.2016.06.008, 2016.

Szymczycha, B., Kłostowska, Ż., Kuliński, K., Winogradow, A., Jakacki, J., Klusek, Z., Grabowski, M., Brodecka-Goluch, A., Graca, B., Stokowski, M., Koziorowska, K., and Rak, D.: Deep submarine groundwater discharge indicated by pore water chloride anomalies in the Gulf of Gdańsk, southern Baltic Sea, E3S Web of Conferences, 54, 00035, https://doi.org/10.1051/e3sconf/20185400035, 2018.

https://doi.org/10.5194/egusphere-2026-519
Preprint. Discussion started: 4 February 2026


Taniguchi, M., Dulai, H., Burnett, K. M., Santos, I. R., Sugimoto, R., Stieglitz, T., Kim, G., Moosdorf, N., and Burnett, W. C.: Submarine groundwater discharge: updates on its measurement techniques, geophysical drivers, magnitudes, and effects, Frontiers in Environmental Science, 7, https://doi.org/10.3389/fenvs.2019.00141, 2019.

Taylor, M. H., Dillon, W. P., and Pecher, I. A.: Trapping and migration of methane associated with the gas hydrate stability zone at the Blake Ridge Diapir: new insights from seismic data, Marine Geology, 164, 79–89, https://doi.org/10.1016/S0025-3227(99)00128-0, 2000.

Timmers, P. H. A., Widjaja-Greefkes, H. C. A., Ramiro-Garcia, J., Plugge, C. M., and Stams, A. J. M.: Growth and activity of ANME clades with different sulfate and sulfide concentrations in the presence of methane, Frontiers in Microbiology, 6, https://doi.org/10.3389/fmicb.2015.00988, 2015.

Ulyanova, M., Sivkov, V., Kanapatskij, T., Sigalevich, P., and Pimenov, N.: Methane fluxes in the southeastern Baltic Sea, Geo-Marine Letters, 32, 535–544, https://doi.org/10.1007/s00367-012-0304-0, 2012.

Uścinowicz, S. (Ed.): Geochemistry of Baltic Sea surface sediments, Polish Geological Institute–National Research Institute, Warsaw, 356 pp., 2011.

Vaksmaa, A., Guerrero-Cruz, S., van Alen, T. A., Cremers, G., Ettwig, K. F., Lüke, C., and Jetten, M. S. M.: Enrichment of anaerobic nitrate-dependent methanotrophic 'Candidatus Methanoperedens nitroreducens' archaea from an Italian paddy field soil, Appl Microbiol Biotechnol, 101, 7075–7084, https://doi.org/10.1007/s00253-017-8416-0, 2017.

Varma, D., Hopmans, E. C., van Kemenade, Z. R., Kusch, S., Berg, S., Bale, N. J., Sangiorgi, F., Reichart, G.-J., Sinninghe Damsté, J. S., and Schouten, S.: Evaluating isoprenoidal hydroxylated GDGT-based temperature proxies in surface sediments from the global ocean, Geochimica et Cosmochimica Acta, 370, 113–127, https://doi.org/10.1016/j.gca.2023.12.019, 2024.

Virtasalo, J. J., Schröder, J. F., Luoma, S., Majaniemi, J., Mursu, J., and Scholten, J.: Submarine groundwater discharge site in the First Salpausselkä ice-marginal formation, south Finland, Solid Earth, 10, 405–423, https://doi.org/10.5194/se-10-405-2019, 2019.

Wakeham, S. G., Lewis, C. M., Hopmans, E. C., Schouten, S., and Sinninghe Damsté, J. S.: Archaea mediate anaerobic oxidation of methane in deep euxinic waters of the Black Sea, Geochimica et Cosmochimica Acta, 67, 1359–1374, https://doi.org/10.1016/S0016-7037(02)01220-6, 2003.

Waters, E., Hohn, M. J., Ahel, I., Graham, D. E., Adams, M. D., Barnstead, M., Beeson, K. Y., Bibbs, L., Bolanos, R., Keller, M., Kretz, K., Lin, X., Mathur, E., Ni, J., Podar, M., Richardson, T., Sutton, G. G., Simon, M., Söll, D., Stetter, K. O., Short, J. M., and Noordewier, M.: The genome of Nanoarchaeum equitans: Insights into early archaeal evolution and derived parasitism, Proceedings of the National Academy of Sciences, 100, 12984–12988, https://doi.org/10.1073/pnas.1735403100, 2003.

Weijers, J. W. H., Schouten, S., Hopmans, E. C., Geenevasen, J. A. J., David, O. R. P., Coleman, J. M., Pancost, R. D., and Sinninghe Damsté, J. S.: Membrane lipids of mesophilic anaerobic bacteria thriving in peats have typical archaeal traits, Environmental Microbiology, 8, 648–657, https://doi.org/10.1111/j.1462-2920.2005.00941.x, 2006.

https://doi.org/10.5194/egusphere-2026-519
Preprint. Discussion started: 4 February 2026


Weijers, J. W. H., Lim, K. L. H., Aquilina, A., Sinninghe Damsté, J. S., and Pancost, R. D.: Biogeochemical controls on glycerol dialkyl glycerol tetraether lipid distributions in sediments characterized by diffusive methane flux, Geochemistry, Geophysics, Geosystems, 12, 1–15, https://doi.org/10.1029/2011GC003724, 2011.

Welte, C., Kröninger, L., and Deppenmeier, U.: Experimental evidence of an acetate transporter protein and characterization of acetate activation in aceticlastic methanogenesis of Methanosarcina mazei, FEMS Microbiology Letters, 359, 147–153, https://doi.org/10.1111/1574-6968.12550, 2014.

Werner, F.: Depressions in mud sediments (Eckernfoerde Bay, Baltic Sea), related to sub-bottom and currents, Meyniana, 30, 99–104, 1978.

Wever, Th. F., Abegg, F., Fiedler, H. M., Fechner, G., and Stender, I. H.: Shallow gas in the muddy sediments of Eckernförde Bay, Germany, Continental Shelf Research, 18, 1715–1739, https://doi.org/10.1016/S0278-4343(98)00055-7, 1998.

Whiticar, M. J.: Diagenetic relationships of methanogenesis, nutrients, acoustic turbidity, pockmarks and freshwater seepages in Eckernförde Bay, Marine Geology, 182, 29–53, https://doi.org/10.1016/S0025-3227(01)00227-4, 2002.

Whiticar, M. J. and Werner, F.: Pockmarks: Submarine vents of natural gas or freshwater seeps?, Geo-Marine Letters, 1, 193–199, https://doi.org/10.1007/BF02462433, 1981.

Wickham, H.: ggplot2: Elegant Graphics for Data Analysis, Springer International Publishing, 260 pp., 2016.

Wittenborn, A. K., Bauersachs, T., Hassenrück, C., Käding, K., Wäge-Recchioni, J., Jürgens, K., Arz, H. W., and Kaiser, J.: Nitrosopumilus as main source of isoprenoid glycerol dialkyl glycerol tetraether lipids in the central Baltic Sea, Frontiers in Microbiology, 14, https://doi.org/10.3389/fmicb.2023.1216130, 2023.

Wood, D. E., Lu, J., and Langmead, B.: Improved metagenomic analysis with Kraken 2, Genome Biology, 20, 257, https://doi.org/10.1186/s13059-019-1891-0, 2019.

Yu, T., Fu, L., Wang, Y., Dong, Y., Chen, Y., Wegener, G., Cheng, L., and Wang, F.: Thermophilic Hadarchaeota grow on long-chain alkanes in syntrophy with methanogens, Nature Communications, 15, 6560, https://doi.org/10.1038/s41467-024-50883-z, 2024.

Zehnder, A. J. B. and Brock, T. D.: Anaerobic methane oxidation: occurrence and ecology, Applied and Environmental Microbiology, 39, 194–204, https://doi.org/10.1128/aem.39.1.194-204.1980, 1980.

Zell, C., Kim, J.-H., Hollander, D., Lorenzoni, L., Baker, P., Silva, C. G., Nittrouer, C., and Sinninghe Damsté, J. S.: Sources and distributions of branched and isoprenoid tetraether lipids on the Amazon shelf and fan: Implications for the use of GDGT-based proxies in marine sediments, Geochimica et Cosmochimica Acta, 139, 293–312, https://doi.org/10.1016/j.gca.2014.04.038, 2014.

Zeng, Z., Chen, H., Yang, H., Chen, Y., Yang, W., Feng, X., Pei, H., and Welander, P. V.: Identification of a protein responsible for the synthesis of archaeal membrane-spanning

https://doi.org/10.5194/egusphere-2026-519
Preprint. Discussion started: 4 February 2026


GDGT lipids, Nature Communications, 13, 1545, https://doi.org/10.1038/s41467-022-29264-x, 2022.

Zhang, Y. G., Zhang, C. L., Liu, X.-L., Li, L., Hinrichs, K.-U., and Noakes, J. E.: Methane Index: A tetraether archaeal lipid biomarker indicator for detecting the instability of marine gas hydrates, Earth and Planetary Science Letters, 307, 525–534, https://doi.org/10.1016/j.epsl.2011.05.031, 2011.

Zhang, Z., Shan, H., Feng, X., Jia, Z., Jiang, L., Wang, S., and Zhu, C.: Review of research progress on the impact of submarine groundwater discharge on pockmark formation and evolution, Journal of Marine Science and Engineering, 13, 1070, https://doi.org/10.3390/jmse13061070, 2025.

Zinke, L. A., Glombitza, C., Bird, J. T., Røy, H., Jørgensen, B. B., Lloyd, K. G., Amend, J. P., and Reese, B. K.: Microbial organic matter degradation potential in Baltic Sea sediments is influenced by depositional conditions and in situ geochemistry, Applied and Environmental Microbiology, 85, e02164-18, https://doi.org/10.1128/AEM.02164-18, 2019.